

Habitable Worlds Observatory (HWO): Living Worlds Working Group: The Search for Life on Potentially Habitable Exoplanets

Co-Chairs: Giada Arney¹, Niki Parenteau²; **Sub-Group Co-Chairs:** Natalie Hinkel³, Eric Mamajek⁴, Joshua Krissansen-Totton⁵, Stephanie Olson⁶, Edward Schwieterman⁷, Sara Walker⁸; **Steering Committee:** Kevin Fogarty², Ravi Kopparapu¹, Jacob Lustig-Yaeger⁹, Mark Moussa¹, Sukrit Ranjan¹⁰, Garima Singh¹¹, Clara Sousa-Silva¹²

¹*NASA Goddard Space Flight Center, Greenbelt, MD, USA*

giada.n.arney@nasa.gov

²*NASA Ames Research Center, Moffett Field, CA, USA*

³*Louisiana State University, Baton Rouge, LA, USA*

⁴*Jet Propulsion Laboratory, California Institute of Technology, Pasadena, CA, USA*

⁵*University of Washington, Seattle, WA, USA*

⁶*Purdue University, West Lafayette, IN, USA*

⁷*University of California at Riverside, Riverside, CA, USA*

⁸*Arizona State University, Tempe, AZ, USA*

⁹*Johns Hopkins University Applied Physics Laboratory, Baltimore, MD, USA*

¹⁰*University of Arizona Lunar and Planetary Laboratory, Tucson, AZ, USA*

¹¹*Gemini North Observatory, Hilo, HI, USA*

¹²*Bard College, Red Hook, NY, USA*

Contributing Authors: Ruslan Belikov (NASA Ames Research Center), Maxwell Frissell (University of Washington), Samantha Gilbert-Janziek (University of Washington), Vincent Kofman (University of Oslo), Natasha Latouf (NASA Goddard Space Flight Center), Mary Anne Limbach (Jet Propulsion Laboratory), Rhonda Morgan (Jet Propulsion Laboratory), Christopher Stark (NASA Goddard Space Flight Center), Armen Tokadjian (Jet Propulsion Laboratory), Anna Grace Ulises (University of Washington), Nicholas Wogan (NASA Ames Research Center), Mike Wong (Carnegie Science), Amber Young (NASA Headquarters)

Endorsed by: Eleonora Alei (NASA Goddard Space Flight Center), Natalie Allen (Johns Hopkins University), Narsreddy Anugu (Georgia State University), David Arnot (The Open University), Reza Ashtari (Johns Hopkins University-Applied Physics Laboratory), Amedeo Balbi (Università di Roma Tor Vergata, Italy), Komal Bali (ETH Zurich), Sarah Barbosa (Universidade Federal do Ceará), Jacob Bean (University of Chicago), Ruslan Belikov (NASA Ames Research Center), Katherine Bennett (Johns Hopkins University), Alan Boss (Carnegie Science), Kara Brugman (Arizona State University), Zachary Burr (ETH Zurich), José A. Caballero (Centro de Astrobiología CSIC-INTA), Douglas Caldwell (SETI Institute), Oliver Carey (Brown University), Aarynn Carter (Space Telescope Science Institute), Jessie Christiansen (Caltech/IPAC), Ligia F Coelho (Cornell University), Giuseppe Conzo (Gruppo Astrofili Palidoro), Jaime Crouse (Johns Hopkins University/NASA Goddard Space Flight Center), Nicolas Crouzet (Kapteyn Astronomical Institute, University of Groningen, The Netherlands), Ruben Joaquin Diaz (NSF NOIRLab), Jamie Dietrich (Arizona State University), Steven Dillmann (University), Luca Fossati (Space Research Institute, Austrian Academy of Sciences), Kevin France (University of Colorado), Megan Gialluca (University of Washington), Ana Ines Gomez de Castro (Universidad Complutense de Madrid), Darío González Picos (Leiden Observatory), Kenneth Goodis Gordon (University of Central Florida), Olivier Guyon (University of Arizona, NAOJ and ABC), Caleb Harada (UC Berkeley), Sonny Harman (NASA Ames Research Center), Xinchuan Huang (SETI Institute & NASA Ames Research Center), Chris Impey (University of Arizona), Markus Janson (Stockholm University), Berger Jean-Philippe (IPAG, Université Grenoble Alpes, CNRS), Renaud Joe (University of Maryland / NASA Goddard), Jens Kammerer (European Southern Observatory), Theodora Karalidi (University of Central Florida), Preethi Kapoor (Indian Institute of Astrophysics), James Kasting (Penn State University), Finnegan Keller (Arizona State University), Alen Kuriakose (KU Leuven, Belgium), Adam Langeveld (Johns Hopkins University), Eunjeong Lee (EisKosmos (CROASAEN), Inc.), Mercedes López-Morales (Space Telescope Science Institute), Evelyn Macdonald (University of Vienna), Jack Madden (Blue Marble Space Institute of Science), Elena Manjavacas (Space Telescope Science Institute), Melinda Soares-Furtado (UW-Madison), Drew Miles (California Institute of Technology), David Montes (UCM, Universidad Complutense de Madrid), Faraz Nasir Saleem (Egyptian Space Agency (EgSA)), Eric Nielsen (Department of Astronomy, New Mexico State University), Sarah Peacock (UMBC/NASA Goddard Space Flight Center), Andreas Quirrenbach (Landessternwarte, U Heidelberg), Patricio Reller (University College London), Ignasi Ribas (Institute of Space Sciences (ICE, CSIC) & Institute of Space Studies of Catalonia (IEEC)), William Roberson (New Mexico State University), Blair Russell (Chapman University), Farid Salama (NASA Ames Research Center), Arnaud Salvador (German Aerospace Center (DLR)), Aniket Sanghi (Caltech), Gaetano Scandariato (INAF), Everett Schlawin (University of Arizona), Laura Silva (INAF-OATs, Italy), Christopher Stark (NASA Goddard Space Flight Center), Sarah Steiger (Space Telescope Science Institute), Tomas Stolker (Leiden University), Johanna Teske (Carnegie Science), Thaddeus Komacek (University of Oxford), Christopher Theissen (UC San Diego), Armen Tokadjian (Jet Propulsion Laboratory), Martin Turbet (LMD, LAB, IPSL, CNRS), MaggieBeth Turcotte (NASA Goddard Space Flight Center (CRESST/SURA)), Vincent Van Eylen (UCL), Connor Vancil (UCSB), Mariela C. Vieytes (Instituto de Astronomía y Física del Espacio (IAFE, CONICET-UBA) Argentina), Iva Vilović (Leibniz Institute for Astrophysics Potsdam (AIP)), Austin Ware (Arizona State University), Jessica Weber (Jet Propulsion Laboratory), Megan Weiner Mansfield (University of Maryland)

1. Abstract

The discovery of a biosphere on another planet would transform how we view ourselves, and our planet Earth, in relation to the rest of the cosmos. We now know Earth is one planet among eight circling our sun; our sun is part of a swirling galaxy of over one hundred billion other suns; and our galaxy is one of untold billions in the universe. While we do not yet know how many – if any – other biospheres exist on the countless worlds orbiting countless other suns, we stand at the precipice of a new era of discovery, enabled by powerful new facilities able to peer across the light years into the atmospheres of planets similar to our own. *This article is an adaptation of a science case document (SCDD) developed for the NASA Astrophysics Flagship mission the Habitable Worlds Observatory (HWO) Science, Technology, and Architecture Review Team (START) Living Worlds Working Group.*

2. Science Goal

Are Earth-like global biospheres common or rare in the galaxy?

“Inspired by the vision of searching for signatures of life on planets outside our solar system... the priority recommendation in the frontier category for space is a large IR/O/UV telescope...” - Astro2020

In recent years, astronomers have constrained the frequency of rocky planets orbiting in their stars’ habitable zones – the region around stars where “Earth-like” conditions and surface liquid water are possible. It is estimated that about one fifth of all stars in our galaxy may have a rocky planet in their habitable zones. Yet, despite knowing the general frequency of planets that might be Earth-like, we do not yet know how many of these worlds actually host habitable conditions. Further, we can only speculate about the fraction of habitable planets that actually host life. The Habitable Worlds Observatory (HWO) will be the first facility ever designed to address the millennia-old question “Are we alone?” By placing the first constraints on the frequency of habitable – and inhabited – planets, HWO’s large aperture and robust instrument suite may help us understand just how alone we are – or discover our universe is teeming with other living worlds.

“If planets like Earth are rare, our own world becomes even more precious. If we do discover the signature of life on another planetary system, it will change our place in the universe in a way not seen since the days of Copernicus.” - Astro2020

3. Science Objective

Discover biosignatures on exoplanets in a false positive/false negative framework, or discover statistically

meaningful limits for null results.

HWO will offer an unprecedented platform to search for remotely observable signs of life, termed “biosignatures,” in the spectra of exoplanets. Life impacts our planet in innumerable ways. Astrobiologists frequently speak of life as a planetary process – one that both modifies and is modified by its environment (Fig. 1). Yet when observing planetary points of light from across the light years, only a small subset of countless life’s impacts on its planet will be remotely observable: those that result from planet-wide, global processes.

Every potential biosignature that we detect must be carefully considered in the context of its environment to mitigate against being confused by abiotic “false positive” mimics. The amount of any gas that we can measure in a planetary atmosphere is the result of competition between source and sink processes. We must obtain enough information about the environment to determine whether a given gas is present because it has a high production rate in an environment with strong sinks, or whether it can be explained by a modest, abiotic production rate in an environment with smaller sinks. These considerations were outlined in the 2022 Biosignatures Standards of Evidence (SoE) Workshop and white paper (Meadows et al. 2022) wherein the authors presented a generalized framework consisting of five scientific questions that would guide the evaluation of a claim of life detection corresponding to both biosignature detection and interpretation. The Living Worlds SCDD is designed to ensure that HWO has the capabilities to follow each step outlined in this standards of evidence framework.

Astrobiologists frequently speak of looking for atmospheres in chemical disequilibrium when seeking biosignatures on exoplanets. Chemical disequilibrium is a state in which two or more chemical species that are incompatible coexist, and it can be quantified by the available free energy in the system (e.g., Krissansen-Totton et al. 2016; Wogan & Catling 2020). Oxygen and methane are examples of gases that coexist in chemical disequilibrium in modern Earth’s atmosphere. Oxygen radicals rapidly destroy methane – its lifetime in Earth’s atmosphere is only about 10 years – so robust continual production is required to explain its presence. Observing chemical disequilibrium on an exoplanet can suggest life (e.g., Hitchcock & Lovelock 1967), because disequilibria can be challenging to maintain through slow, abiotic production rates of gases – although exceptions exist (Wogan & Catling 2020), so planetary context must be considered to rule out false positives (Fig. 2).

Given that our planet is our only example of a habitable world with life, strategies to search for life on exoplanets generally start with considerations of how to detect life on Earth (e.g., Sagan et al. 1993). Yet our planet has not always looked the way it does today (Fig. 1). In the same way that peering across interstellar distances will reveal diverse ex-

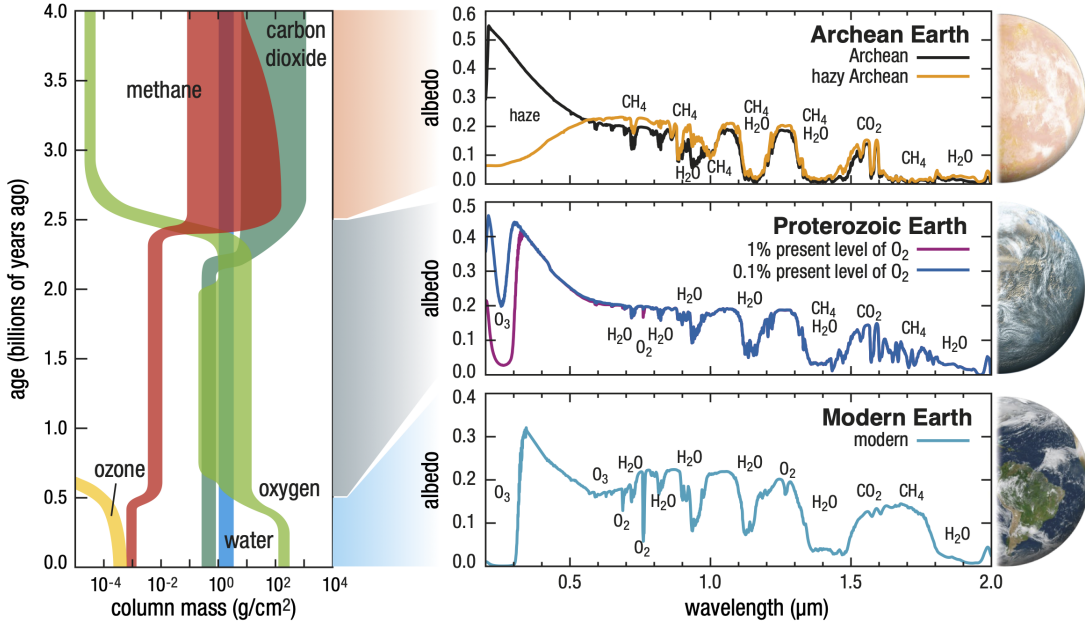


Fig. 1.— Biosignatures and habitability indicators of Earth through time reflect how life on our planet has co-evolved with its environment. The biosignatures of Earth through time are a useful minimum set of spectral features to seek on exoplanets with HWO.

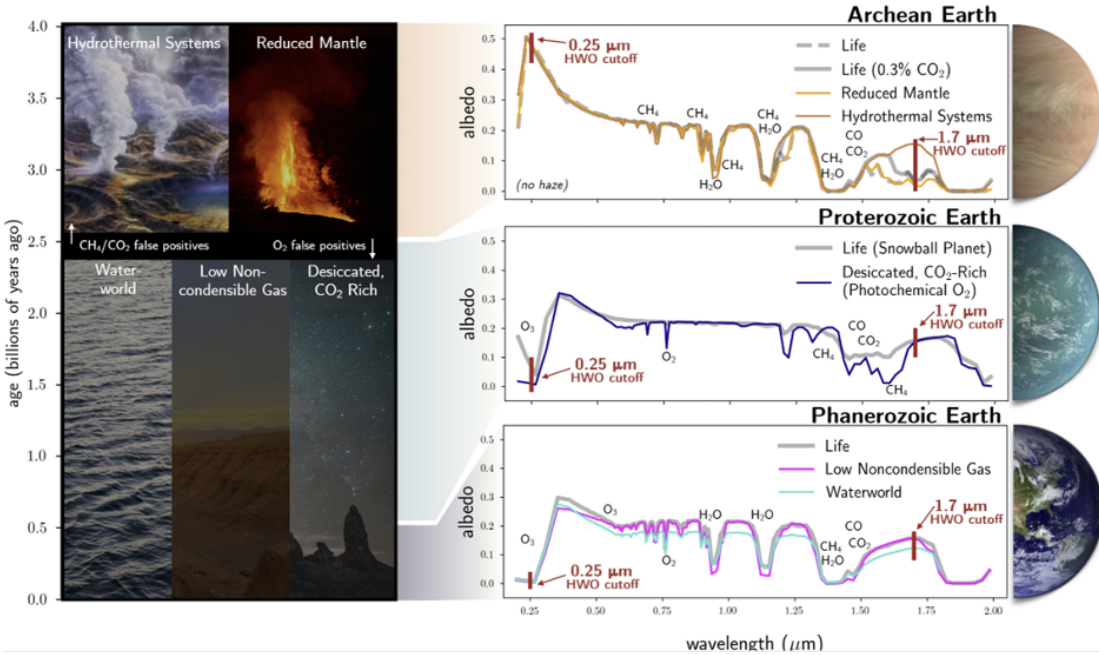


Fig. 2.— Biosignatures must be considered in the context of their environments to rule out false positives. Possible false positive planets are shown, with relevant spectral features labeled. False positives relevant to oxygenated planets are on the bottom (Phanerozoic, or modern, Earth and Proterozoic Earth); those relevant to anoxic planets (Archean Earth) are on the top. Figure by Samantha Gilbert-Janizek (UW).

oplanets unlike our own, looking back through geological time shows us different types of dominant biospheres and environments that prevailed on our world over Earth's history. Thus, if we want to search for signs of life on "Earth-like" exoplanets, we should, at minimum, design an observatory capable of detecting signs of life on exoplanets similar to the different faces of Earth over its history. The dominant biosignatures of our planet have varied considerably over Earth history (Fig. 3), requiring a wide wavelength range spanning from the NUV to the NIR to characterize each inhabited phase of our planet over geological time. An observatory not capable of detecting the dominant, planet-wide spectral features indicative of habitability and life on planets analogous to Earth through time will run the risk of being under-designed to meet its eponymous central goal.

Briefly, Earth's major geological periods encompass the following.

The earliest eon of Earth history, the **Hadean** (before 4 billion years ago) is very poorly constrained due to an extremely sparse geological record. Yet Earth was likely habitable by the end of the Hadean (Harrison et al. 2005), and there is evidence that life may have arisen during this period (e.g., Bell et al. 2015; Nutman et al. 2016). Large impacts may have induced transient highly reducing atmospheric states (Zahnle et al. 2010), which may have been important for prebiotic chemistry. Photochemical and lightning reactions in the Hadean atmosphere may also have contributed chemical precursors to life (e.g., Wogan et al. 2023) and metabolically useful molecules (Kasting 2014).

The **Archean** (4-2.5 billion years ago) boasted an anoxic atmosphere and a thriving microbial, anaerobic biosphere. It is likely that Archean Earth's atmosphere was rich in greenhouse gases (e.g., carbon dioxide, CO₂ and methane, CH₄) to warm our planet to hospitable temperatures under the illumination of our fainter sun at this time period (75%-80% the modern solar luminosity). Atmospheric methane abundances, in particular, may have been 2-3 orders of magnitude greater than today (Pavlov et al. 2000) due to robust production of this gas by methane-producing methanogen microorganisms (Woese & Fox 1977; Ueno et al. 2006) and a long atmospheric lifetime in an oxygen-poor environment. However, methane can also be produced by abiotic processes, so care must be taken when interpreting this gas as a biosignature (e.g., Krissansen-Totton et al. 2022). The abundances of other carbon-bearing species are important pieces of contextual information required to interpret methane as a biosignature in anoxic atmospheres: specifically, the abundances of CH₄, CO₂, and CO must be well-constrained, as must the photochemical context generated by the UV spectrum of the host star (Thompson et al. 2022; Schwieterman et al. 2019).

For planets with high amounts of CH₄ relative to CO₂ (e.g. CH₄/CO₂ ratios in excess of ~0.2), organic haze

particles can form (e.g., Trainer et al. 2006), dramatically alternating the planet's spectral appearance at UV-blue wavelengths, its climate (given that hazes have an anti-greenhouse effect), and its surface habitability (given that hazes are strong UV absorbers) (Arney et al. 2016, 2017, 2018). Organic haze may have transiently existed in Earth's atmosphere during the Archean (e.g., Zerkle et al. 2012), challenging the notion that all "Earths" will be the "pale blue dots." Hazy Archean Earth, appearing a pale orange to remote observers, is arguably the most "alien" planet for which we have geochemical data, reminding us of the importance of designing an observatory capable of characterizing planets with a wide variety of properties dissimilar to modern Earth.

The **Proterozoic** eon (2.5 billion years ago – 541 million years ago) began with the marked rise of oxygen (O₂) in our planet's atmosphere, irreversibly altering our planet's remotely observable characteristics in numerous ways. Additionally, the rise of oxygen and its photochemical byproduct, ozone (O₃), provided a powerful ultraviolet shield that may have eased the transition of life from the seas onto land. Yet during the mid-Proterozoic, oxygen levels may have been as low as 0.1% of the present atmospheric level (Planavsky et al. 2014; Lyons et al. 2014, 2021). Methane atmospheric abundances may likewise have been suppressed to low levels, possibly low enough to render methane's spectral features largely invisible to an observatory like HWO (Olson et al. 2016), though the strongest band at 1.65 μm could be observable for CH₄ abundances modestly higher than modern Earth's (e.g., ~10 ppm compared to modern Earth's ~1.6 ppm). An additional biosignature that could be sought on Proterozoic-like exoplanets is N₂O (e.g., Buick 2007; Schwieterman et al. 2022), although N₂O's relatively weak spectral features < 2 μm and these features' overlap with H₂O features suggest that only high N₂O abundances (~100-1,000 ppm) might be detected (Tokadjian et al. 2024).

Based on what is known about the mid-Proterozoic, a strong spectral feature from O₃ in the near UV (NUV) is the best – and possibly only – remotely observable sign of life for a facility like HWO. The best opportunity to capture a disequilibrium biosignature (e.g., between O₃ and CH₄, or O₃ and N₂O) requires wavelength coverage from ~0.25 μm to ~1.7 μm to fully capture the O₃ Hartley band (~0.3 μm cutoff), and strong 1.65 μm CH₄ band in its entirety, and possibly the strongest NIR N₂O bands (1.52, 1.68, 1.78 μm). It cannot be overstated: the mid-Proterozoic, which lasted for about a billion years, represents a planetary archetype that would pose a formidable challenge for life-detection on a planet analogous to our own. An observatory under-designed to meet this challenge runs the risk of a false negative detection of life (e.g., Reinhard et al. 2017) on similar exoplanets. False negative detections of life on weakly

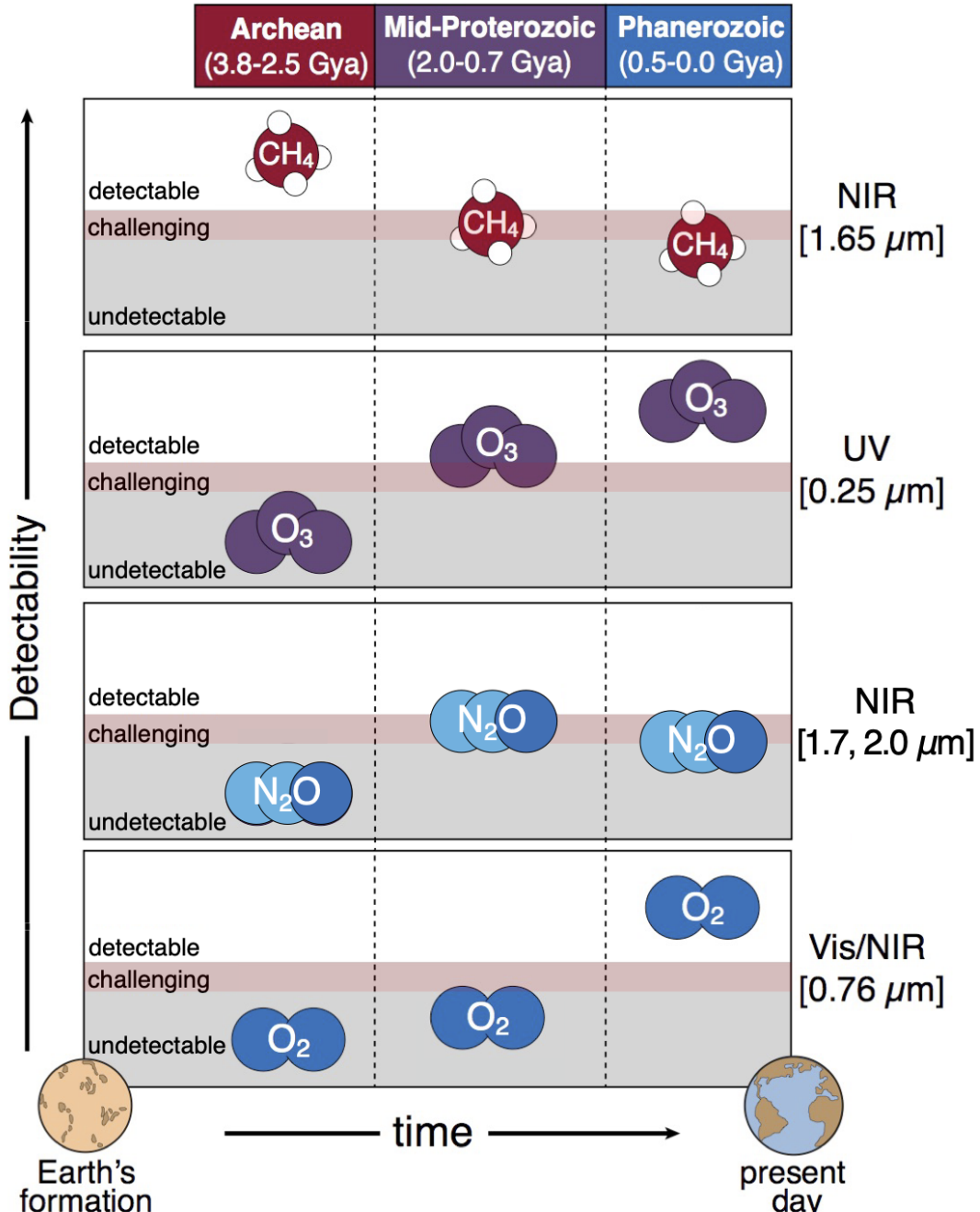


Fig. 3.— The dominant biosignatures of Earth, and their detectability, have varied over our planet's geological history. Different photochemistries around different stars can also alter the relative detectability of biosignatures. A wavelength range from the NUV to the NIR ensures that the dominant biosignatures over Earth history can be detected on exoplanets.

oxygenated planets similar to mid-Proterozoic Earth may pose a greater obstacle to searches for life beyond the Earth than false positive detections of life on uninhabited planets: given that oxygen is a highly reactive gas, there are numer-

ous barriers to its accumulation in planetary atmospheres even if a biosphere is producing it (e.g., Lyons et al. 2014).

Modern, or Phanerozoic Earth (541 million years ago – present) has been scrutinized as an analog for exoplanets

(e.g., [Sagan et al. 1993](#); [Robinson & Reinhard 2018](#)). Modern Earth is and always will be our best-studied, best understood world, providing invaluable information to inform future mission designs. Important gases in modern Earth's atmosphere include O_2 , O_3 , CH_4 , and CO_2 . While the simultaneous presence of oxygen and methane have been pointed to as an important gas pair indicative of an atmosphere in chemical disequilibrium that is extremely difficult or even impossible to explain without life (e.g., [Hitchcock & Lovelock 1967](#)), methane may be challenging to detect in the atmosphere of a modern Earth twin due to precisely the same process that renders it a valuable biosignature: oxygen radicals sourced from ozone photochemistry destroy methane rapidly, so its photochemical lifetime in the atmosphere is only about 10 years, and it is present at a scant part-per-million abundance with minor spectral impact in the HWO wavelength range. In absence of a methane detection, the only way to rule out the main false positive process that can produce oxygen around sun-like stars is to constrain other atmospheric constituents, including background gases, total atmospheric pressure, and surface composition/climate (see below). However, different photochemical consequences in the atmospheres of planets around other types of stars add nuance to this picture, and it may be easier to detect oxygen and methane together for modern Earth-like planets orbiting stars of lower mass than the sun (e.g., [Segura et al. 2005](#); [Arney 2019](#)).

It has been suggested that our planet entered a new geological epoch for the most recent sliver of Earth history: the **Anthropocene**, a period of significant human impact on the Earth, with various proposed start dates ranging from the Neolithic period to as recently as the last decades. While this period is not officially recognized at present, considering it reminds us that a different type of biosignature, technosignatures, might be possible to remotely detect on exoplanets. While biosignatures are signs of life in general, technosignatures are remotely observable signs of technology.

The reasons for the focus on Earth through time are not purely Earth-centric. Methane-producing metabolisms are relatively simple compared to other biogenic gas-producing metabolisms, and it's reasonable to speculate that they may evolve on other worlds given the probable ubiquity of the necessary substrates (H_2 , CO_2). Indeed, methanogenesis emerged early in Earth's evolution ([Weiss et al. 2016](#); [Wolfe & Fournier 2018](#)). Similarly, oxygen biosignatures from photosynthesis may also be ubiquitous since the substrates (H_2O , CO_2) would be widely available on a habitable exoplanet. Compared to geochemical electron donors such as H_2 , which are typically in low supply in limited environments, the distribution of H_2O that serves as an electron donor for oxygenic photosynthesis would allow for global-scale proliferation in surface environments. However, it

must be noted that the 'metabolic machinery' of the photosynthetic subsystems is complex and it's not a foregone conclusion that oxygenic photosynthesis would evolve on exoplanets.

With that said, it would be more surprising to discover that all living worlds look like Earth through time than it would be to discover worlds radically different from Earth. Therefore, while we should ensure that HWO is capable of sensing signs of life on planets like Earth, it is also important to design an observatory with sufficiently robust capabilities that maximize our chances of observing and correctly interpreting biosignatures on planets with different histories and alien (in every sense of the word) biospheres. The history of exoplanet discoveries reminds us that we must be prepared for the unexpected as we consider the existence of exoplanets not represented by solar system analogs (e.g., Hot Jupiters, mini Neptunes, super Earths) and discovery of unexpected processes (e.g., planetary migration). There is no reason to think that our first observations of potentially habitable and inhabited planets will be any less surprising. If anything, we should expect the challenges of interpreting living worlds to be significantly greater than the challenges of interpreting other kinds of processes, especially given our singular world for comparison. Meeting this challenge demands an observatory with the most robust capabilities possible (e.g., wide wavelength range, large aperture, small inner working angle, etc.).

There are numerous biosignature gases to be sought (e.g., [Seager et al. 2012](#); [Kaltenegger 2017](#); [Schwieterman et al. 2018](#); [Catling et al. 2018](#)), as well as other planetary features that will help us interpret those features in the context of their environments. A useful Objective to bound HWO capabilities is capturing ozone in the NUV and methane, carbon dioxide, and carbon monoxide in the NIR near $1.7\ \mu m$, for as many targets as possible. In between these wavelengths, other key gases can be observed: O_2 , H_2O , CO_2 , O_2-O_2 , and others (Fig. 1-4). Here, we describe key categories of biosignature gases and other spectral features required to understand those detections in the proper context.

3.1. Biosignatures in Oxidized Atmospheres

Molecular oxygen (O_2) has generally been considered the highest priority biosignature gas to seek in exoplanet atmospheres (e.g., [Meadows 2017](#)). The byproduct of our planet's dominant metabolism, oxygenic photosynthesis, O_2 has profoundly changed our atmosphere – and spectrum – over Earth's geological history. While other more primitive forms of anoxygenic photosynthesis are possible, they are limited by availability of reductants (e.g., H_2 , H_2S , Fe_2^+) and would only be detectable via surface biosignatures of their photosynthetic pigments. Oxygenic photosynthesis, meanwhile, uses cosmically ubiquitous compounds:

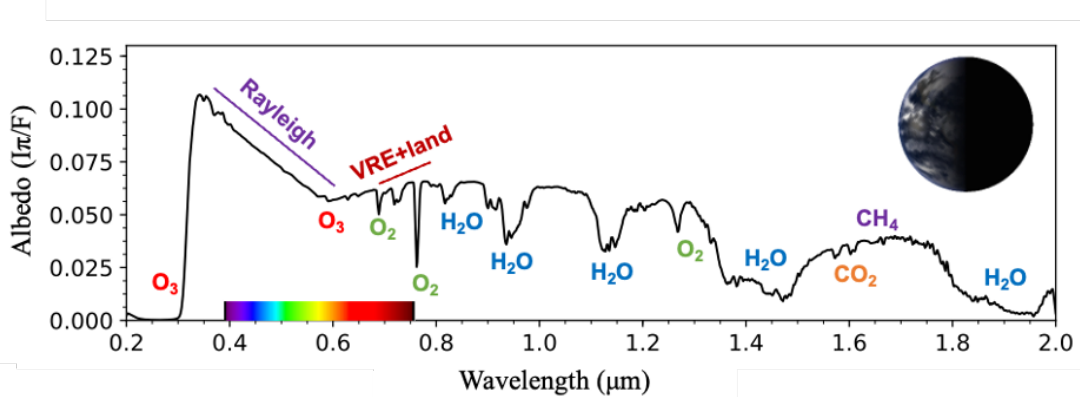
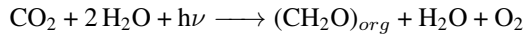
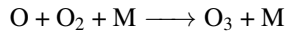
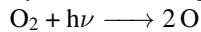


Fig. 4.— Spectral features of Modern Earth at quadrature phase (half illumination). This figure is reproduced with minor modifications from Schwieterman et al. (2018a) under Creative Commons Attribution License CC-BY 4.0. Figure modifications include labels of additional gas features, an inset of a simulated Earth at half illumination, and an inset color bar indicating the visible wavelength range.

H_2O , starlight ($\text{h}\nu$), as well as CO_2 , which is expected to occur generally on terrestrial planets:



Ozone is a photochemical byproduct of atmospheric O_2 . The reactions that produce and destroy O_3 on Earth are generally called the Chapman reactions (Chapman 1930):



Here, M is an inert molecule or neutral atom that can carry away excess energy and momentum. Naturally, given that these reactions depend on photochemistry, different stars may be more or less efficient at generating – or destroying – ozone (e.g., Segura et al. 2003; Grenfell et al. 2014; Arney 2019). Additionally, energetic particles from stellar activity can deplete O_3 (Tabataba-Vakili et al. 2016; Tilley et al. 2019). In a general sense, understanding the photochemical context of an atmosphere is critical for evaluating biosignatures.

As described above, ozone is a critical indicator of weakly oxygenated planets such as Proterozoic Earth, because it has a strong spectral feature at NUV wavelengths even for planets with little O_2 . This feature may be the only observable biosignature at HWO wavelengths for planets similar to the mid-Proterozoic, so access to it is critical for guarding against false negative detections of life on weakly oxygenated planets with low amounts of atmospheric CH_4 . Additionally, changes in seasonal oxygen production on weakly oxygenated planets might be detected by modulations in the strength of NUV ozone feature as a type of temporal biosignature (Olson et al. 2018).

3.1.1. Oxygen biosignature false positives

Detection of O_2 or O_3 in an exoplanet atmosphere would be a watershed moment, but this detection alone would not prove that there is life on the planet, for there are abiotic processes that can produce an atmosphere with detectable O_2 that must be considered (Meadows 2017). Fig. 5 summarizes information on various oxygen false positive scenarios. Most of these false positive scenarios primarily apply to M dwarf stars and could result in massive quantities (i.e., bars) of oxygen through water-loss processes. Such oxygen-rich atmospheres could be identified through detection of O_2 – O_2 collisional induced absorption features (Schwieterman et al. 2016). More relevant to the sun-like (F/G/K) stars that represent the majority of the HWO target stars is false positive oxygen generated by the following mechanisms:

- On planets with low non-condensable gas inventories (e.g., N_2), water vapor can more easily reach the upper atmosphere (Wordsworth & Pierrehumbert 2014) where it can be photolyzed to generate false positive O_2 , followed by loss to space of the lightweight liberated H. Background non-condensable gases can be constrained by observing a planet’s Rayleigh scattering slope, as well as through observations of pressure broadening of spectral features (Young et al. 2024). The background gas abundance and composition may also be inferred by elimination of other plausible background gas constituents (Hall et al. 2023). However, access to NIR wavelengths ($\sim 1.7 \mu\text{m}$) is necessary to distinguish between a N_2 background and CO background, since the latter could indicate a photochemical oxygen biosignature false positive.

- Planets with extremely deep surface oceans may accumulate significant abiotic oxygen via H escape since the pressure overburden of \sim 50+ Earth oceans suppresses oxygen sinks (Krissansen-Totton et al. 2021). Such a scenario can be ruled out by land detection, which puts an upper limit on ocean depth. Land detection requires robust surface characterization capabilities.
- Planets in a moist or runaway greenhouse state can experience O₂ accumulation from elevated H loss following H₂O photolysis. Such planets are likely to occur closer to their stars than the conservative habitable zone boundaries (e.g., Kopparapu et al. 2013). Constraints on orbit as well as CO₂ and H₂O abundance will be required to rule out these false positives.
- Planets with high CO₂ abundances and low abundances of hydrogen-bearing molecules can experience O₂ buildup due to the breakdown of the OH-mediated catalytic cycles that recombine photolyzed CO₂ (Gao et al. 2015). This mechanism would also accumulate abundant CO, so upper limits on CO abundance can rule out this false positive. Additionally, the detection of hydrogen-bearing species in the planet’s atmosphere can rule out this false positive.

Note that many of the photochemical false positives for oxygen have recently been eliminated by model intercomparisons, reducing the ambiguity of oxygen as a biosignature (Ranjan et al. 2020; Ranjan et al. 2023). Note that all of these oxygen false positive scenarios would be strongly disfavored by a simultaneous detection of atmospheric methane. This is because the implied kinetic disequilibrium is extremely challenging to explain without large methane fluxes, which would not be expected for any of the scenarios above, or indeed for any plausible abiotic process. While it is challenging to detect oxygen and methane simultaneously in the photochemical context of modern Earth orbiting the sun, the photochemical lifetime of methane is longer around lower mass stars such as M dwarfs (Segura et al. 2005) and K dwarfs (Arney 2019), so these stars likely offer better prospects for simultaneously detecting this key gaseous disequilibrium pair.

3.2. Biosignatures in Anoxic Atmospheres

For anoxic atmospheres like Archean Earth, atmospheric methane is the most promising biosignature candidate. Archean Earth likely had similar rates of methane production to the modern Earth (Kharecha et al. 2005; Sauter et al. 2020), but this gas’s longer photochemical lifetime in an anoxic atmosphere would have enabled orders of magnitude more methane to accumulate in the atmosphere of

Archean Earth compared to modern Earth, enhancing its detectability.

3.2.1. Methane biosignature false positives

With that said, methane—just as with oxygen—can be produced by abiotic processes, so careful consideration of potential “false positives” is needed before a biological source can be inferred.

On modern Earth, biological methane production outpaces abiotic production at a rate of about 65:1 (Etiope & Sherwood Lollar 2013). Studies have investigated the maximum amount of abiotic methane that might be produced on a terrestrial planet (e.g., see Fig. 6; Krissansen-Totton et al. 2018; Wogan & Catling 2020; Thompson et al. 2022). These studies find that known abiotic processes are typically unable to produce atmospheres with abundant CH₄ and CO₂ due to the redox disequilibrium of these gases, so this pair of gases is critical to observe together when interpreting CH₄ as a biosignature on anoxic worlds. Another gas relevant to interpretation of biogenic methane is CO because CO would be produced by volcanoes on a planet with a highly reducing mantle able to produce abundant volcanic CH₄. Thus, CH₄ and CO₂ together, with a high CH₄/CO abundance ratio, would be strong evidence pointing towards biogenic methane for anoxic planets. The possibility of methane false positives highlights the need for sufficient NIR capabilities to constrain abundances of CO₂, CH₄, and CO.

In addition to the methane flux-producing false positive scenarios above, methane-rich atmospheres from Titan-analogs, post-impact atmospheres, or sub-Neptunes could also be mistaken for an Archean-like biosphere. Possible observational strategies to rule out such false positives are described in Fig. 5.

3.3. Other Biosignatures

Nitrous oxide (N₂O) is produced by life on Earth through microbial nitrogen metabolisms, which are, in turn, enabled by the presence of abundant oxidants produced by oxygenic photosynthesis. The modern N₂O atmospheric abundance is low, precluding detection with HWO: 330 ppb (270 ppb pre-industrial). However, past phases of Earth history may have experienced higher amounts of N₂O. The N₂O abundance in the Proterozoic atmosphere could have been much greater than today because of the limited ocean oxygenation during that time period, which would have limited trace metals necessary for converting N₂O to N₂ gas via biological metabolism (e.g., Knowles 1982; Pinto et al. 2021). A Proterozoic Earth planet orbiting a G-type star can potentially accumulate a N₂O volume mixing ratio (VMR) of up to 100 ppm (VMR = 10⁻⁴) while a planet around a K-type star has an upper limit of 1000 ppm (VMR = 10⁻³) due to

	False positive scenario	Contextual information needed to rule out false positive	Implied requirements for HWO
False positives for oxygen/ozone biosignatures (Phanerozoic and Proterozoic Earth)	Low non-condensable inventory (Wordsworth and Pierrehumbert 2014)	Infer background gas by elimination and total pressure Rayleigh slope + pressure broadening (Hall et al. 2023; Young et al. 2024)	0.3 – 1.7 μ m SNR = 10-40 (40 for strong constraints) (Hall et al. 2023) R = 140 in VIS, 70 in NIR
	Waterworld scenario (Krissansen-Totton et al. 2021)	Land detection via surface spectrum (Ulises et al. 2025, in prep) or time-resolved mapping (e.g. Lustig-Yaeger et al. 2018)	0.3-1.1 μ m; SNR > 20 (Ulises et al. 2025) 1 hour SNR > 10 (Lustig-Yaeger et al. 2018)
	Runaway greenhouse atmosphere (Kasting and Pollack, 1983, Icarus)	CO ₂ and H ₂ O abundances, total pressure via Rayleigh scattering and O ₂ -O ₂ CIA. Habitability indicators.	Likely NIR coverage to 1.7 μ m, SNR > 10.
	Photochemical false positive (Harman et al. 2018; Ranjan et al. 2020)	A priori unlikely for F/G/K dwarfs. Stellar UV, CO ₂ , CO to confirm	NIR coverage to 1.7 μ m. Sufficient spectral resolution to disentangle CO ₂ and CO near 1.6 μ m.
False positives for methane biosignatures (Archean Earth)	Reduced mantle degassing (Wogan et al. 2020)	Well-constrained abundances of CH ₄ , CO, and CO ₂	NIR coverage to 1.7 μ m SNR > 10
	Warm Titan-analog (Krissansen-Totton et al. 2022)	Bulk density, orbital configuration + evolutionary models	Orbital constraints; mass and radius estimates
	Hydrothermally generated methane (Thompson et al. 2022)	Well-constrained CH ₄ abundances, stellar UV	NIR coverage to 1.5 μ m and SNR = 20-40
	Transient impact-generated atmosphere (Zahnle et al. 2020) or C-rich sub-Neptune (Benneke et al. 2024).	Constrain mean molecular weight, CO abundance. Habitability indicators. Planetary age for large impact plausibility.	NIR coverage to 1.7 μ m SNR>10

Fig. 5.— Types of biosignatures and false positives for different types of environments.

the lower UV flux (a major N₂O sink) from a K vs G star (Schwieterman et al. 2022).

Numerous other biosignatures may be possible (e.g. biogenic sulfur gases; Domagal-Goldman et al. (2011)) and many others (e.g., Seager et al. 2016). Any potential biosignature relevant to HWO must: 1) have absorption features in the HWO wavelength range; 2) accumulate to detectable quantities in a relevant planetary and photochemical context – or have a detectable photochemical byproduct distinguishable from abiotic processes; 3) be studied rigorously to understand potential false positive scenarios. The dominant biosignatures of Earth through time remain the best studied biosignatures for obvious reasons, but we cannot exclude the possibility of other biosignatures on exoplan-

ets. Additional work is needed to mature our understanding of other promising biosignatures, especially given that many have incomplete linelists, incomplete reaction rates, or other deficiencies (e.g., Seager et al. 2016).

3.4. Corroborating Habitability

Many of the biosignature false positive scenarios described above could be ruled out by directly confirming surface habitability. Water, while not a biosignature itself, is a critical indicator of planetary habitability. While other solvents have been proposed for life, water has key advantages (Pohorille & Pratt 2012) and it is the most common solvent and polyatomic molecule in the universe. Indeed, the very definition of the habitable zone is the region around stars

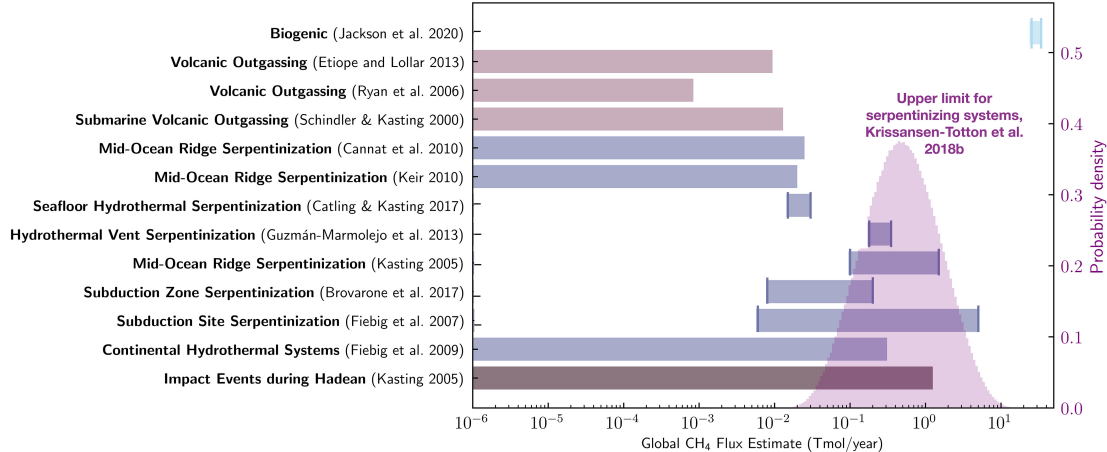


Fig. 6.— Abiotic sources of methane compared to Earth’s modern biogenic flux, which is more rapid than all abiotic sources. Reproduced with permission from Thompson et al. (2022).

where surface liquid water is most probable. Gas-phase water can be detected through its atmospheric spectral features. Direct detection of surface liquid water may be possible on a subset of targets through observation of specular reflection off an ocean (“glint”) (e.g., [Robinson et al. 2010](#); [Lustig-Yaeger et al. 2018](#)), although glint observations will be complicated by the coronagraph inner working angle (IWA) given the necessity of the planet being in or near crescent phase.

As discussed above, carbon dioxide is a critical part of the planetary context required to interpret methane or organic haze as biosignatures in anoxic atmospheres. Carbon dioxide is also an important greenhouse gas and is detectable on some Earth through time analogs, so constraints on this gas are important for understanding the greenhouse gas budget of a planetary atmosphere.

4. Physical Parameters

[Astro2020](#) suggests that HWO examine ~ 25 terrestrial planets in their stars’ habitable zones for signs of habitability and life. This sample size would guarantee seeing at least one planet with biosignatures at 95% confidence, if the frequency of inhabited planets with observable global biospheres is 10% of all candidates. As another example, if, instead, we suppose that 10% of rocky habitable zone planets represent an Earth twin at a random point in Earth’s evolution, we must observe 33 planets to observe biosignatures at 95% confidence because 11% of the “Earths” in the sample will be Hadean-like and uninhabited. More generally, the number of candidate exoplanets (N_{ec}) required to constrain the fraction of planets with a given characteristic x (η_x) at a given confidence level (c) can be written as:

$$N_{ec} = \log(1 - c) / \log(1 - \eta_x). \quad (1)$$

We can visualize what this means in Fig. 7.

It is also useful to think about what this means in the case of a null detection. If we examine 25 candidate spectra and do not see signs of life, then we can say that the frequency of habitable planets with observable signs of life is $< 10\%$ of candidate planets in the nearby universe at 95% confidence, placing the first ever upper limit on the frequency of observable biospheres in the cosmos. Fig. 8 qualitatively summarizes what we might infer about the frequency of planets with various characteristics given different underlying frequencies of true biosignatures and false positives.

It is also useful to consider how our confidence in interpreting biosignatures may vary based on the spectral type of the parent star. Planets orbiting stars similar to the sun will likely experience star-planet evolutionary histories more akin to Earth around the sun compared to planets orbiting stars with pronounced differences, e.g., dramatically shorter lifetimes, extreme early stellar activity, etc. Our confidence is bolstered in interpreting biosignatures in the atmospheres of planets orbiting sun-like stars. Additionally, more types of biosignature false positives have been identified for planets orbiting later-type stars (e.g., M dwarfs) compared to sun-like stars (e.g., [Meadows 2017](#)). We concur with the guidance in [Astro2020](#) to focus the search for habitable planets around sun-like stars as the highest priority targets. However, planets orbiting stars with dramatically different star-planet evolutionary histories compared to the Earth around the sun offer a valuable comparative planetology perspective. These lower mass stars should not be excluded from the target list. We recommend that the target star list place the highest priority on sun-like stars (G and K dwarfs are the highest priority; F dwarfs are second priority given their lower numbers and on-average greater distances to the Earth presenting SNR and IWA is-

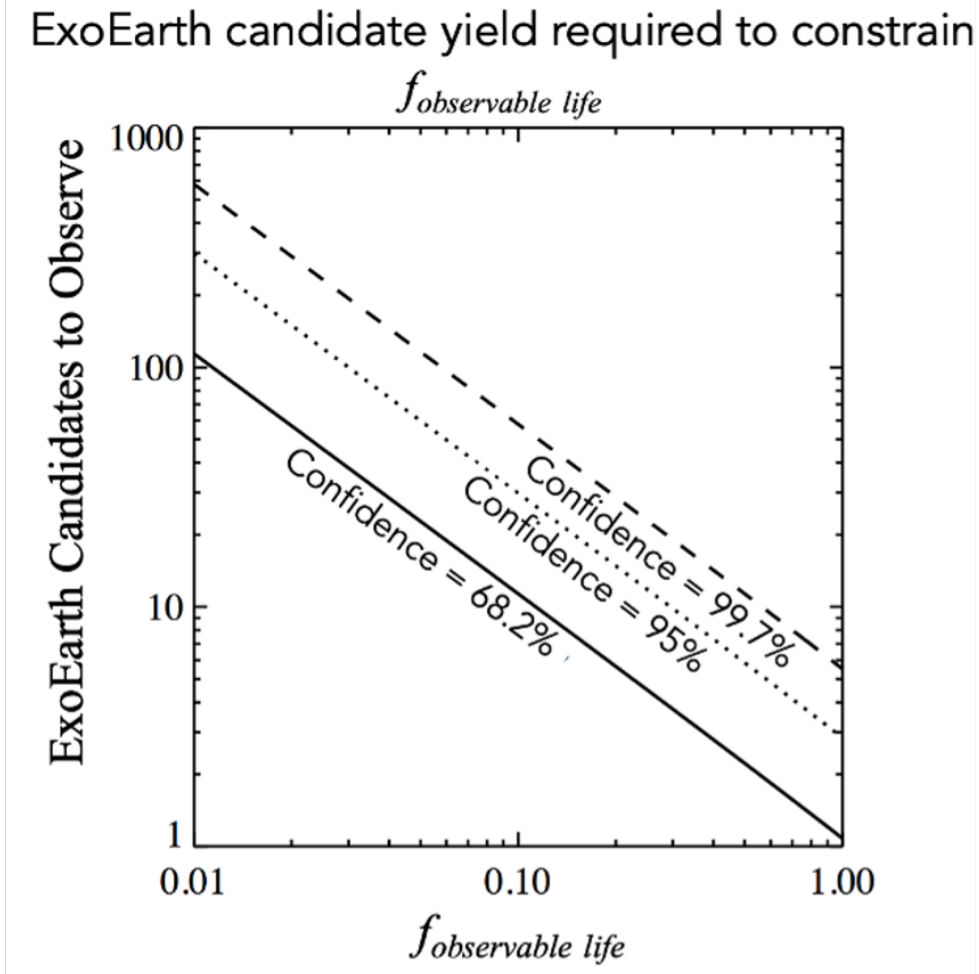


Fig. 7.— The number of candidate planets that must be observed to constrain various fractions of planets with observable life/biosignatures for given confidence levels. Credit: Christopher Stark.

sues). More ambitious plans could also include A dwarfs, but given the low numbers of these stars, their shorter lifetimes, and their greater average distances, we recommend that M dwarfs be prioritized over A dwarfs.

4.1. Key Physical Parameters

Below, we describe the information we require from a planet to place important constraints on key properties relevant to the search for habitability and life.

Water (H_2O)

Detect abundance of atmospheric water vapor to order of magnitude precision for abundances comparable to modern Earth ($\sim 1\%$ by volume).

Rationale: Provide context for biosignature interpretation, constraints on planetary greenhouse warming, and information about habitability.

Oxygen (O_2)

Detect abundance of atmospheric oxygen, a key biosignature, to order of magnitude precision for abundances comparable to Modern Earth's (21% by volume).

Rationale: Key biosignature of modern and Proterozoic Earth.

Ozone (O_3)

Detect abundance of atmospheric ozone to 1-2 orders of magnitude precision for photochemical abundances consistent with Proterozoic Earth's oxygen level (i.e., corresponding to 0.1% present atmospheric level for O_2).

Rationale: Key biosignature of modern and Proterozoic Earth.

IF Given a Statistically Robust Sample of HZ Planetary Spectra

"False Positive" Biosignatures		"True Positive" Biosignatures	
		rare	common
common			
	<p>Prediction: O_2/O_3 detected preferentially in Venus zone (due to H escape) or other contexts incompatible with habitability. False positive indicators (e.g., O_4) detected.</p> <p>Interpretation: Detectable global biospheres are rare in the solar neighborhood. Abiotic processes mimicking some biosignatures are common.</p> <p>Confidence: Medium.</p>	<p>Prediction: O_2, O_3, and CH_4 detection in contexts consistent with varied origins (e.g., inside and outside HZ). False positive indicators present in some targets.</p> <p>Interpretation: Abiotic processes mimicking some biosignatures are common. More detailed spectral analysis is required for compelling targets.</p> <p>Confidence: Low to Medium.</p>	
rare	<p>Prediction: No detection of O_2, O_3, or levels of CH_4 on a temperate planet indicative of biological activity. No detection of alternative biosignatures.</p> <p>Interpretation: Detectable global biospheres are rare in the solar neighborhood.</p> <p>Confidence: High.</p>	<p>Prediction: Detection of O_2, O_3, CH_4, and/or alternative biosignatures on multiple HZ planets. No detection of abiotic O_2/O_3 in the Venus zone or other contexts. No false positive indicators.</p> <p>Interpretation: Detectable global biospheres are common in the solar neighborhood.</p> <p>Confidence: Medium to High.</p>	

Fig. 8.— Testable hypotheses about the prevalence of detectable biosignatures and their false positives in the solar neighborhood predicated on how intrinsically common or rare true or false positive biosignatures are. While we often focus on the upper right quadrant, where both biosignatures and their associated false positives are common and individual detections may be ambiguous, other possibilities could be confirmed or refuted even with a capable mission, so long as a statistically robust sample of planets is examined both inside and outside (e.g., interior to) the habitable zone, and false positive disambiguators like O_4 can be detected or excluded.

Methane (CH_4)

Detect abundance of atmospheric methane to order of magnitude precision for abundances comparable to a low-abundance Archean Earth (500 ppm).

Rationale: Key biosignature for Archean Earth; constraints on greenhouse warming; can rule out oxygen false positives.

Organic Haze

Detect organic haze if present in anoxic atmospheres for $CH_4/CO_2 > 0.2$.

Rationale: Secondary biosignature of Archean Earth; habitability implications.

Carbon Dioxide (CO_2)

Detect abundance of atmospheric carbon dioxide to order of magnitude precision for abundances comparable to a low-abundance Archean Earth ($\sim 1\%$ of the total atmosphere by volume).

Rationale: Needed for false positive interpretation on anoxic planets; constraints on greenhouse warming.

Carbon Monoxide (CO)

Place an upper limit on CO if present at $< 1\%$ or 0.01 bar abundances.

Rationale: Needed for false positive interpretation on anoxic planets.

Nitrous Oxide (N_2O)

While N_2O Proterozoic Earth abundances (1-10 ppm) would be challenging to detect, even this amount of N_2O is suggestive of habitability and life. A more realistic goal is to detect N_2O at abundances corresponding to an upper limit for a Proterozoic Earth-like planet around a G-star (100 ppm) or K-star (1000 ppm). Minimum requirement: detect N_2O at 10^{-3} near $1.4\ \mu m$.

Rationale: Secondary biosignature of Proterozoic Earth.

Surface Pressure (or implied N_2)

Constrain absolute surface pressure to a factor of a few (0.25-0.5 bar).

Rationale: Needed for false positive interpretation on oxygen-rich planets and for inferring planetary climate.

Fig. 9 summarizes the physical parameters that must be measured, along with the requisite abundance or upper limit for gases, and number of targets, in order to search for biosignatures and constrain the prevalence of life in the galaxy. For these calculations, we assume some variable X% percentage of habitable zone, Earth-sized planets represent Earth at a random point in its history (11% Hadean, 33% Archean, 44% Proterozoic, and 11% Phanerozoic). Given the atmospheric gases that can be measured, we then calculate the number of targets that must be characterized to rule out an X% prevalence to 95% confidence, as shown in Fig. 7.

For example, for the “Incremental Progress” case, we assume that every HZ Earth-sized planet is an Earth twin (X=100%) but only Phanerozoic-like O_2 levels and Archean-like CH_4 abundances can be identified given the observatory capabilities. Thus Earth twins with Proterozoic-like biosignatures are invisible, and so only 33% + 11% = 44% of Earth twins can be identified. Consequently, $\log(1 - 0.95) / \log(1 - 0.44 * 100\%) = 5$ targets are needed to rule out this prevalence of life to 95% confidence. Crucially, however, without the ability to constrain CO_2 , CO , or surface pressure ($N = 0$ for each of these parameters), then biosignature false positives cannot be ruled out. We achieve a constraint on the prevalence of Earth-like atmospheric abundances, but not a constraint on the prevalence of life, and so progress is deemed “incremental.” This scenario is also deemed incremental because an implausibly high prevalence of Earth-twins is assumed, $X = 100\%$.

Next, we consider the example of the “Breakthrough Progress” case. Here, we intend to test the more conservative hypothesis that only X=10% Earth-sized planets in the habitable zone are Earth twins. For the breakthrough case, we assume we can constrain Phanerozoic-like O_2 , Proterozoic-like O_3 , and Archean-like CH_4 . This means that biosignature gases are detectable for 11% + 44% + 33% = 88% of Earth twins. Furthermore, we assume sufficient capabilities to contextualize any potential biosignatures via constraints on CO , CO_2 , H_2O , surface pressure. This ability to rule out biosignature false positives for the Earth through time means that $\log(1 - 0.95) / \log(1 - 0.88 * 10\%) = 33$ targets are needed to confirm or rule out a 10% prevalence of life in the galaxy. The “Substantial Progress” and “Major Progress” scenarios explore in-between cases with different assumed prevalences (X%) and capabilities

to identify biosignature false positives.

Note that this SCDD does not discriminate between single and multi-star systems (binaries and higher order). Multi-star systems are present in the current HWO target list, so we expect that most of the science described in this document will be conducted on single as well as binary stars. The presence of multi-star targets is beneficial to this SCDD: they not only increase the expected science yield of the mission, but also likely increase the SNR and spectral coverage of the average planet target. This is because the average FGK star system is closer to us than the average FGK single-star system, which increases the SNR through greater planet photon flux and improves NIR coverage due to larger working angle. Furthermore, the nearest FGK star system to us (Alpha Centauri) is an unusual outlier – it is 2.4 times closer than the next nearest FGK star. This means that, roughly speaking, we expect at least 2.4 easier working angle and $2.4^2 = 5$ times more photons from a planet orbiting Alpha Centauri than a similar planet orbiting any other FGK star. If HWO sensitivity to biomarkers is limited by planet flux or inner working angle, then HWO would be sensitive to fainter biomarkers on such a planet. If biomarkers are common but faint, then Alpha Centauri could mean the difference between HWO finding life or not. In addition to the yield and sensitivity advantages, binary stars also allow comparative science between single- and binary- star systems: for example, studies of how binarity affects habitable world formation, evolution, dynamics, etc. (For one example of this, see Elizabeth Newton’s SCDD.)

5. Description of Observations

A wavelength range spanning from $\sim 0.25 - 1.7 \mu m$ provides access to the dominant biosignatures on Earth over its inhabited history according to our best understanding of current geological evidence, in addition to habitability markers and biosignature false positive indicators. Notably, access to these wavelengths also will provide the ability to follow the “decision tree” strategy outlined in Young et al. (2024) for characterizing Earth-like exoplanets (Fig. 10). This strategy allows observers to classify planets based on phases of Earth history by searching for the dominant biosignatures of Earth through time – and their false positive indicators. Such strategies are especially important to consider given that coronagraphs can only observe spectra within a 10-20% bandpass at a time.

Of course, it will not be possible to access this entire wavelength range for every HWO target. Fig. 11 shows the distribution of potential target stars from the Habitable Worlds Observatory Preliminary Input Catalog (HPIC) (Tuchow et al. 2024) as shaded curves. Overlain on this are the stars for which various wavelengths are theoretically accessible for an IWA of $2\lambda/D$ and $3.5\lambda/D$ for a planet

Physical Parameter	State of the Art	Incremental Progress (Enhancing) (visible only)	Substantial Progress (Enabling) (visible only)	Major Progress (Visible, NIR)	Breakthrough (NUV, visible, NIR)	Breakthrough + (NUV, visible, NIR, more targets)
Short Summary	0 exo-Earths directly observed in reflected light around FGK stars Some around M stars may be observed by ELTs	Hypothesis tested: 100% of rocky HZ planets represent an Earth twin at a random point in Earth's evolution: 44% of "Earths" characterizable for this scenario. ** No context for biosignature interpretation, so no constraint on life's prevalence.	Hypothesis tested: 50%* of rocky HZ planets represent an Earth twin at a random point in Earth's evolution: 44% of "Earths" characterizable for this scenario. No context for biosignature interpretation so no constraint on life's prevalence.	Hypotheses tested: 25% of HZ planets represent an Earth twin at a random point in Earth's evolution: 44% of "Earths" characterizable for this scenario. No ability to characterize Proterozoic-like planets.	Hypotheses tested: 10% of rocky HZ planets represent an Earth twin at a random point in Earth's evolution: 88% of "Earths" characterizable for this scenario. Ability to characterize biosignatures for all of Earth's inhabited history. Context for biosignature interpretation.	Hypotheses tested: 5% of rocky HZ planets represent an Earth twin at a random point in Earth's evolution: 88% of "Earths" characterizable for this scenario. Ability to characterize biosignatures for all of Earth's inhabited history. Context for biosignature interpretation.
	Gases Measured N/A	Gases Measured Modern H ₂ O + O ₂ . High Archean CH ₄ .	Gases Measured Modern H ₂ O + O ₂ . High Archean CH ₄	Gases Measured Low H ₂ O, Modern O ₂ , Archean CH ₄ , biosignature inference through false positive indicators (CO upper limit, CO ₂ detection)	Gases Measured Low H ₂ O, Modern + low Proterozoic O ₂ (via O ₃), Archean and high Proterozoic CH ₄ , biosignature inference through false positive indicators (CO upper limit, CO ₂ detection, surface pressure)	Gases Measured Low H ₂ O, Modern + low Proterozoic O ₂ (via O ₃), Archean and high Proterozoic CH ₄ , biosignature inference through false positive indicators (CO upper limit, CO ₂ detection, surface pressure)
H ₂ O	N = 0	N=5	N=12	N=26	N=33	N=67
	A = N/A	A=0.01	A=0.01	A=3x10 ⁻⁴	A=3x10 ⁻⁴	A=3x10 ⁻⁴
O ₂	N = 0	N=5	N=12	N=26	N=33	N=67
	A = N/A	A=PAL [†]	A=PAL	A=PAL	A=PAL	A=PAL
CH ₄	N = 0	N=5	N=12	N=26	N= 33	N=67
	A = N/A	A=500 ppm	A=500 ppm	A=100 ppm	A=100 ppm	A=100 ppm
CO ₂	N = 0	N = 0	N = 0	N=26	N=33	N=67
	A = N/A	A = N/A	A = N/A	A = 1%	A=1%	A=1%
CO	N=0	N=0	N=0	N=26	N=33	N=67
	UL=N/A	UL=N/A	UL=N/A	UL = 10%	UL = 10%	UL = 1%
O ₃	N=0	N = 0	N = 0	N = 0	N = 33	N=67
	A = N/A	A = N/A	A = N/A	A = N/A	A = 3x10 ⁻⁸	A = 3x10 ⁻⁸
P _{surface} (or implied N ₂)	N=0	N = 0	N = 0	N = 0	N=33	N=67
	A = N/A	A=N/A	A=N/A	A=N/A	A = 0.5 bar	0.25 bar

*Half of solar system habitable zone planets are an Earth twin.

†Present Atmospheric Level (PAL).

Fig. 9.— Physical parameters and number of targets required for biosignature search. Columns denote progress in search for life and corresponding constraints on the prevalence of life in the galaxy. Rows denote required physical parameter measurements and number of accessible targets. A denotes required abundance (mixing ratio) constraint, whereas UL denotes required mixing ratio upper limit. N denotes the number of targets. Note that this does not imply that all gases must be precisely constrained for all N targets, merely that the possibility of obtaining constraints via long integrations exists for the most promising targets in the N-sized sample. N is the number of planets that must be observed to rule out each column's prevalence scenario (X%) to 2 sigma (95% confidence) based on the fraction of Earth history on which life would have been observable for the scenario.

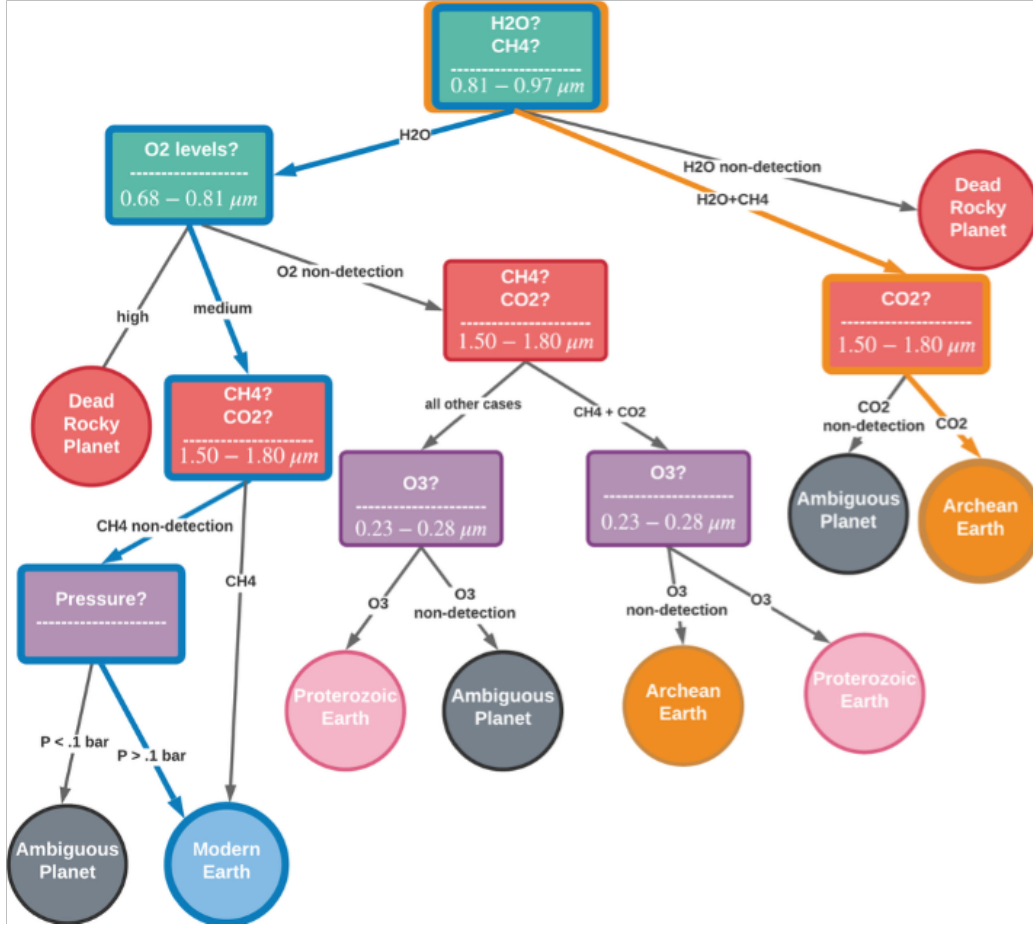


Fig. 10.— A decision tree strategy for characterizing Earth-like exoplanets (Young et al. 2024). This tree indicates which gasses to observe, and in which order, to detect the biosignatures of Earth through time and rule out relevant false positives. The blue path was followed in spectral retrievals of Young et al. (2024) to categorize modern Earth, and the orange path for Archean Earth. Reproduced with permission from Young et al. (2024).

with Earth's equivalent equilibrium temperature around every star for telescopes with 6.5, 8, and 10 m diameters. Unsurprisingly, smaller IWA values and larger telescope apertures provide access to more targets and a wider wavelength range. Ozone in the NUV is the most readily accessible biosignature for the most number of targets based on the parameters considered here. In practice, the number of stars that can actually be accessed for a given architecture will be considerably smaller when exposure time, etc is accounted for.

Morgan et al. (2024) presented HWO yield sensitivities in the NIR and NUV and showed the sensitivity of the NIR yield, in particular, to the IWA and aperture. Of note, the paper concludes that “The NIR achieves 25 exo-Earths characterized only at 9-m aperture and 20 mas IWA, which corresponds to $1 \lambda/D$.” While these are clearly aggressive numbers, our point is that it is very evident that aperture and

IWA are key parameters that will drive the yield of planets that are successfully searched for biosignatures and false positive indicators.

Additional rationale for observation requirements is provided below for each key gas.

Water (H_2O)

We require observations of water to constrain planetary habitability. SNR = 6 for bandpasses centered between 0.86 and 0.95 is sufficient to provide a strong H_2O detection for a modern Earth-like water abundance at $R = 140$ and a 20% bandpass (Fig. 12; Latouf et al. (2023a,b)).

Fig. 13 shows detectability of the water vapor feature near $0.9 \mu m$ for varied water vapor abundances that might represent variability of water on our planet over its history from Latouf et al. (2023a). For the lowest water abundances assumed, SNR = 12 is required to provide a strong detection

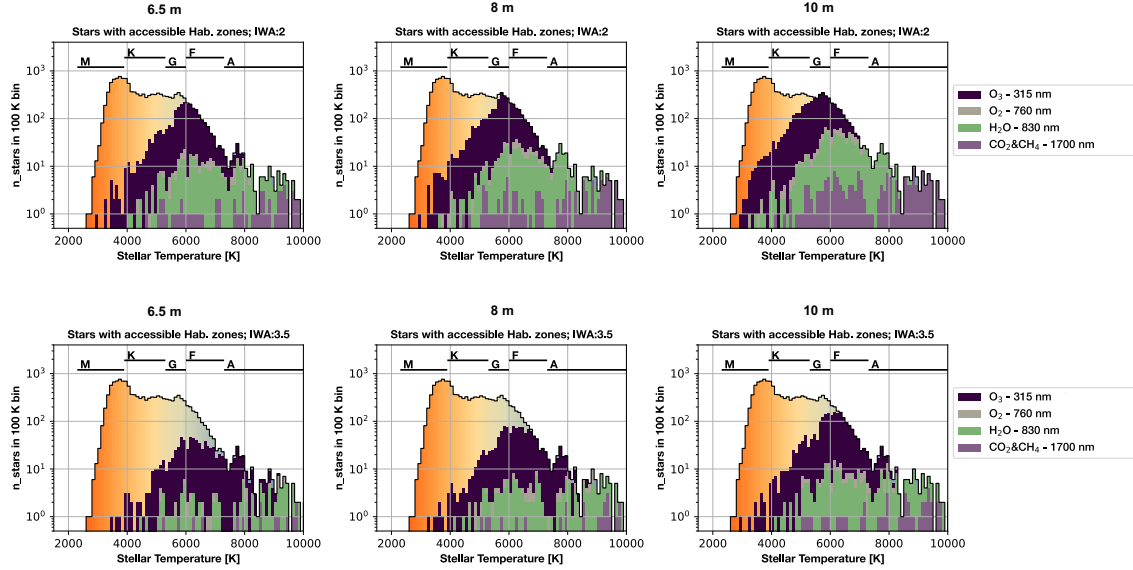


Fig. 11.— The distribution of potential target stars from the Habitable Worlds Observatory Preliminary Input Catalog (HPIC; [Tuchow et al. \(2024\)](#)) as shaded curves. The orange gradient represents all stars in the target volume while the dark purple, gray, green, and light purple colored regions indicate those systems with accessible HZs at the wavelength cutoff given in the legend. Overlain on this are the stars for which various wavelengths are accessible for an IWA of $2\lambda/D$ (top) and $3.5\lambda/D$ (bottom) for an orbiting planet with Earth’s equivalent equilibrium temperature for telescopes with 6.5, 8, and 10 m diameters. Figure and simulations by Vincent Kofman.

at $R = 140$ and 20% bandpasses.

Oxygen (O_2)

Oxygen’s strongest feature, the “A Band” absorbs at 0.76 μm , with secondary features at 1.27, 0.69, and 0.63 μm . As shown in Figure 10, bandpasses centered between 0.7 and 0.83 μm can achieve a strong detection of O_2 for a spectrum with $R = 140$ and 20% bandpasses at $\text{SNR} > 8$, consistent with findings from the LUVOIR final report. The required resolution, which sets the visible channel resolution, is based on sampling the width of the O_2 A-band.

Ozone (O_3)

Ozone has strong absorption features in the NUV (the Hartley-Huggins bands), and a broad feature at visible wavelengths (the Chappuis band). We consider the Hartley-Huggins NUV band most critical, as it may be the only observable biosignature for a planet similar to mid-Proterozoic Earth; when the Chappuis band is visible, the O_2 A-band will be visible as well.

There has been concern about the overlap of the NUV ozone band and the NUV sulfur dioxide band (SO_2) given that both bands’ absorption starts near 0.33 μm . We investigated the impact of realistic SO_2 in an Earth-like atmosphere on spectral retrievals of ozone using a photo-

chemical model representing Proterozoic Earth with varied SO_2 fluxes. Sulfur dioxide is produced by volcanoes, and a reasonable range for the modern volcanic SO_2 flux has been estimated as $1 - 3.5 \times 10^9$ molecules/cm 2 /s ([Zahnle et al. 2006](#)). However, we find these fluxes do not produce enough SO_2 to impact the planet’s spectrum. A minor SO_2 feature appears for fluxes of 9×10^{10} molecules/cm 2 /s, which is almost a full an order of magnitude higher than a “high” estimate of the Archean SO_2 flux ([Zahnle et al. 2006](#)), when the planet may have been more volcanically active.

Fig. 14 shows retrievals of O_3 and SO_2 for SO_2 fluxes of 9×10^{10} molecules/cm 2 /s (weak SO_2 feature, yellow spectrum) and 9×10^{11} molecules/cm 2 /s (moderate SO_2 feature, blue spectrum), but the latter flux may be implausibly high. Ozone can be retrieved well, but SO_2 remains unconstrained. We emphasize that high abundances of SO_2 may be incompatible with a habitable planet given that high amounts of atmospheric SO_2 such as those required to produce a spectral feature appear to require a planet with little or no surface liquid water ([Loftus et al. 2019](#)). High levels of SO_2 may also generate H_2SO_4 or S_8 aerosols, depending on the atmospheric redox state (e.g., [Hu et al. 2013](#)). The highest levels of SO_2 generate H_2SO_4 aerosols in our simulations (excluded from spectral retrievals), which would

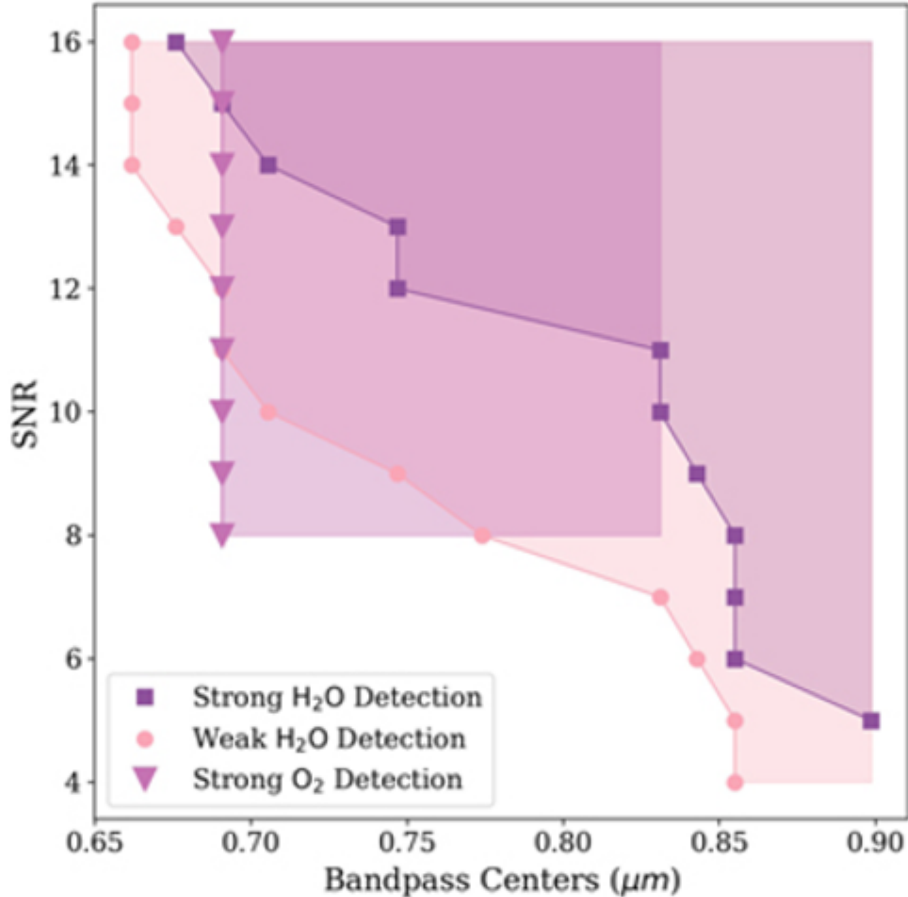


Fig. 12.— Strength of water vapor and oxygen detection as a function of SNR and spectral bandpass center for a 20% bandpass. Reproduced with permission from [Latouf et al. \(2023a,b\)](#).

be an independent flag for high SO_2 abundance. None of our atmospheres generate S_8 hazes, which is expected, because S_8 formation requires anoxic conditions (e.g., [Pavlov & Kasting 2002](#); [Zahnle et al. 2006](#)).

Fig. 15 explores the shortest wavelength required to constrain ozone for 0.1% (top) and 1% (bottom) the present level of O_2 and “high” SO_2 (a surface flux of 10×10^{11} molecules/cm²/s) at SNR = 10. For this scenario, access to wavelengths $> 0.288 \mu\text{m}$ is required to adequately constrain Proterozoic ozone. Independently, [Damiano et al. \(2023\)](#) recommended a short wavelength cutoff of $0.25 \mu\text{m}$ for the best constraints on O_3 .

The short wavelength cutoff

Fig. 16 summarizes the results of our team’s spectral retrieval analyses for the short wavelength coronagraph cutoff. Specifically, we investigate the short wavelength cutoff required to contextualize Earth-through-time biosignatures and rule out known false positives for the case of Proterozoic Earth.

Based on these results, we conclude a short wavelength cutoff of at least $0.25 \mu\text{m}$ is needed to constrain O_3 sufficiently well to confidently detect life on Earth at any time in its history; a more restricted wavelength range would potentially lead to ambiguous findings as known biosignature false negatives given that the NUV O_3 feature may have been the only detectable biosignature in the NUV-NIR for a billion years of Earth’s history.

Nitrous Oxide (N_2O)

[Tokadjian et al. \(2024\)](#) show that with spectral resolution 7/140/70 in the UV/O/IR and SNR = 20, N_2O at an atmospheric fraction of 10^{-3} is reliably constrained for long wavelength cutoff at least $1.4 \mu\text{m}$. However, N_2O at an atmospheric fraction of 10^{-4} is not detectable even for the full wavelength range (up to $1.8 \mu\text{m}$). Given that K dwarfs accumulate more N_2O due to their lower UV flux ([Schwielerman et al. 2022](#)), our best option for detecting N_2O on an Earth-like exoplanet through reflection spectroscopy is to focus on K-type stellar hosts and to use a wavelength

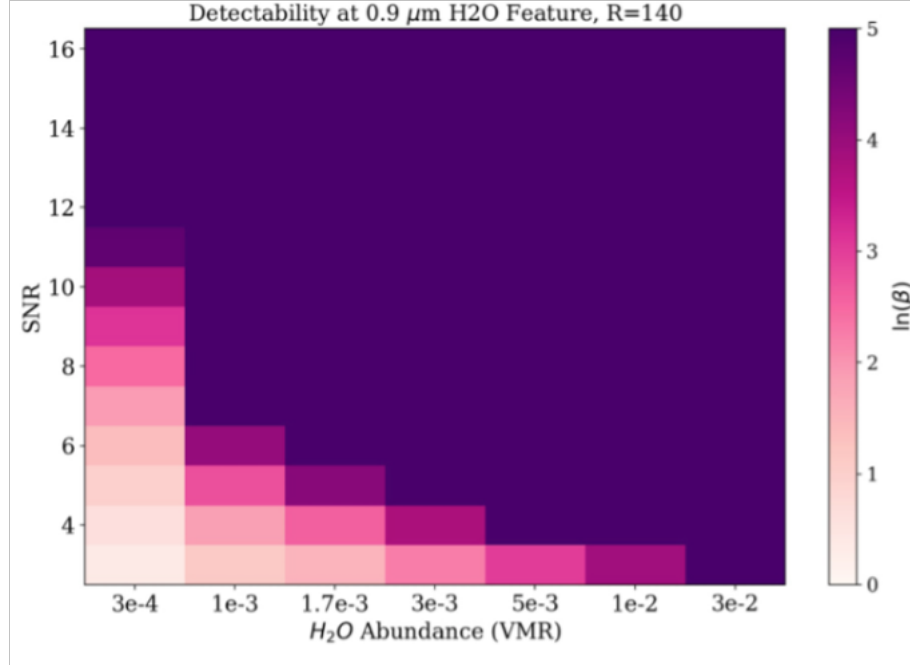


Fig. 13.— SNR required to detect the $0.9 \mu\text{m}$ water vapor feature for varied water abundances. $\ln(b) > 5$ represents a “strong” detection according to the criteria used in Latouf et al. (2023a,b). Reproduced with permission from Latouf et al. (2023a,b).

range that extends to at least $1.4 \mu\text{m}$.

Methane (CH_4)

For modern Earth, methane absorbs weakly near $1.7 \mu\text{m}$, but observing this feature for a modern Earth twin would require extraordinarily high SNR (Young et al. 2024). Methane’s spectral features are stronger, and extend to shorter wavelengths, for planets akin to Archean Earth with higher abundances of CH_4 . Young et al. (2024) shows that methane can be measured near $0.9 \mu\text{m}$ for an Archean-like planet with 1000 ppm CH_4 at $\text{SNR} = 10$. The methane feature near $1.7 \mu\text{m}$ provides additional leverage for constraining methane on Archean-like planets, and it remains the most observable methane band for planets with more moderate CH_4 levels (e.g., 500 ppm), so access to this band remains critical. Our retrieval analyses for CH_4 are summarized in Fig. 17.

Organic Haze

Wavelengths $< 0.5 \mu\text{m}$ provide access to organic haze absorption, which is a broad spectral feature. Future work, especially spectral retrieval modeling of hazy planets, is needed to constrain organic haze observation requirements.

Carbon Dioxide (CO_2)

Modern Earth-like abundances of CO_2 are extremely difficult to constrain (Fig. 17; Young et al. 2024). Fig. 17 shows that Phanerozoic-like CO_2 levels can be constrained to within 2 orders of magnitude if the long wavelength cutoff can be extended to $2 \mu\text{m}$, but this requires $\text{SNR} = 40$ and would require cooling the telescope.

For a planet with higher levels of CO_2 (e.g., Archean Earth, with possibly $\sim 1\%$ atmospheric CO_2 or more), $\text{SNR} = 10$ can place modest constraints on CO_2 , and $\text{SNR} = 20$ can place stronger constraints (Young et al. 2024) via the CO_2 features near $1.6 \mu\text{m}$. Fig. 17 shows that 1% CO_2 requires high SNR (40) to constrain to within 1 order of magnitude, but CO_2 can be constrained to within 2 orders of magnitude for $\text{SNR} = 20$. Even 20% CO_2 requires $\text{SNR} = 20$ to constrain to 1 order of magnitude, but it can be constrained to within 2 orders of magnitude for $\text{SNR} = 10$ for a long wavelength cutoff of $1.7 \mu\text{m}$.

Carbon Monoxide (CO)

Carbon monoxide has absorption features at 1.58 and $2.34 \mu\text{m}$. The $1.58 \mu\text{m}$ feature is weak and partially overlaps an absorption feature from carbon dioxide, making spectral retrievals challenging. Fig. 17 shows that our retrievals were unable to constrain CO in all cases tested; however, a 10^{-1} upper limit is possible for a long wave-

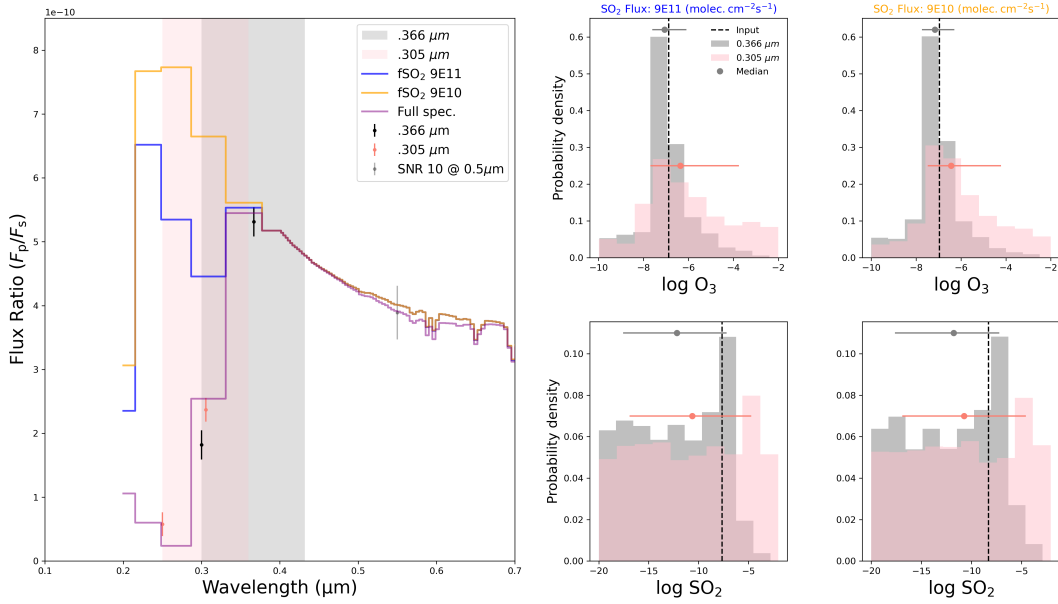


Fig. 14.— SO_2 is unlikely to confuse ozone retrievals in the NUV. The blue and yellow spectra contain no ozone to clearly show the SO_2 absorption at two SO_2 flux levels indicated in the legend; the purple (full) spectrum includes ozone and SO_2 . The fluxes of SO_2 required to produce an SO_2 spectral signature may be implausibly high in an Earth-like photochemical context given that these fluxes are more than 1-2 orders of magnitude higher than modern Earth’s SO_2 flux. Retrievals for two spectral ranges containing two photometric points are included; ozone is constrained by these retrievals, but SO_2 is not. Figure and simulations by Amber Young.

length cutoff $> 1.6 \mu\text{m}$ at $\text{CO} = 50\text{-}500 \text{ ppm}$ for $\text{SNR} > 10$.

The long wavelength cutoff

Fig. 17 summarizes the results of spectral retrieval analyses for the long wavelength coronagraph cutoff. Specifically, we investigate the long wavelength cutoff required to contextualize Earth-through-time biosignatures and rule out known false positives (see above). For the Phanerozoic Earth, we find that detecting atmospheric CO_2 , a potential habitability indicator, would be challenging for any plausible long wavelength cutoff, as would detecting trace amounts of methane. However, access to $> 1.6 \mu\text{m}$ would enable CO -dominated atmospheres to be excluded, thereby ruling out photochemical oxygen false positives. For the Proterozoic Earth, biogenic methane may be detectable if abundances were at the high end of literature estimates ($\sim 100 \text{ ppm}$), and access to $> 1.7 \mu\text{m}$ enables biogenic methane detection even if the achievable SNR in the NIR is poor (~ 10). This is particularly desirable given the opportunity to simultaneously detect O_3 and CH_4 under this high CH_4 scenario, which would be an especially compelling biosignature with no known false positives. Moreover, access to $> 1.6 \mu\text{m}$ enables CO -dominated atmospheres to

be excluded, once again ruling out photochemical oxygen false positives. Finally, for the Archean Earth, both CO_2 and biogenic CH_4 are detectable for all long wavelength cutoffs we considered. However, access to $> 1.6 \mu\text{m}$ is needed to rule out CO -dominated atmospheres, and thereby disfavor methane biosignature false positives produced by a reducing planetary interior.

Based on these results, we conclude a long wavelength cutoff of at least $1.7 \mu\text{m}$ is needed to constrain CO_2 , CH_4 , and CO sufficiently well to confidently detect life on Earth at any time in its history; a more restricted wavelength range would potentially lead to ambiguous findings as known biosignature false positives could not be excluded. Extending the spectrometer to longer wavelengths ($> 1.7 \mu\text{m}$) to measure additional species not considered here would provide additional leverage to characterize unknown exoplanets on planets observable at those wavelengths (i.e., brighter targets), but we do not recommend that this drive observatory thermal design given the challenges associated with a cold telescope.

Other Planetary Properties

Surface temperature and atmospheric pressure are key planetary properties relevant to habitability and planetary

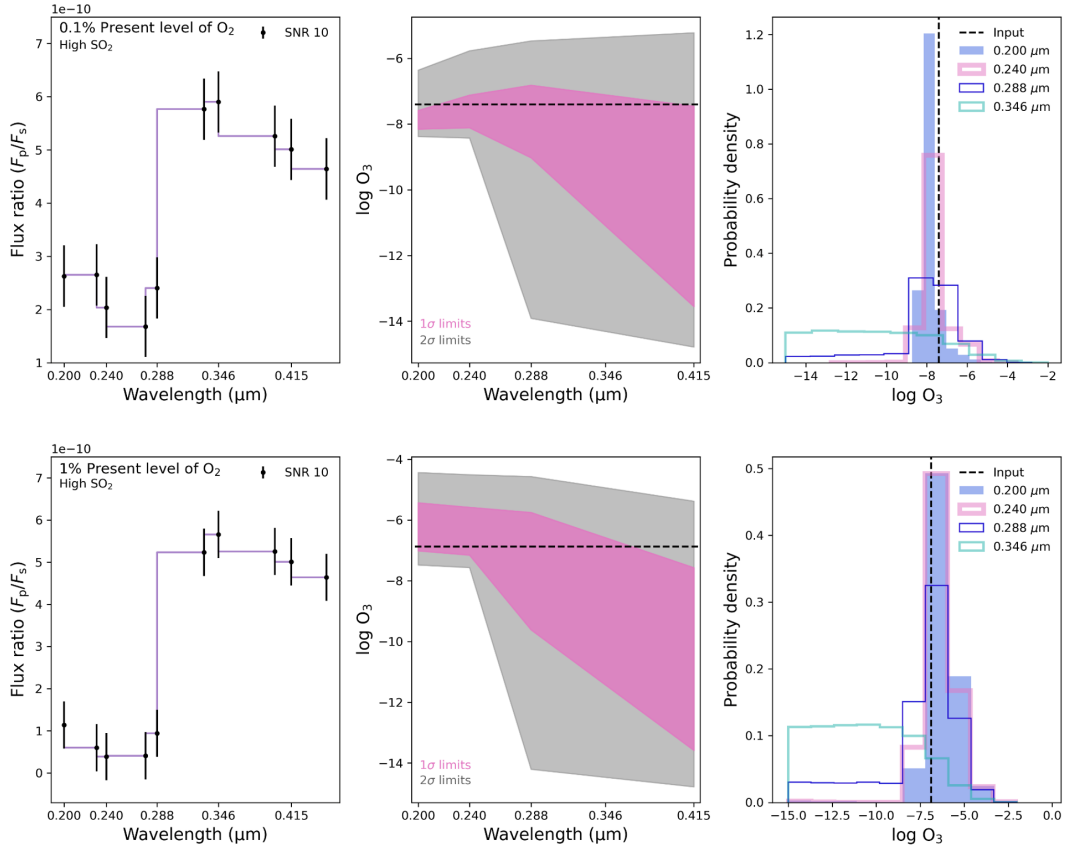


Fig. 15.— Access to wavelengths $< 0.288 \mu\text{m}$ is required to adequately constrain ozone for Proterozoic-like planets. Figure and simulations by Amber Young.

context required to rule out certain false positives such as an oxygen false positive scenario driven by low atmospheric pressures (~ 0.1 bar; [Wordsworth & Pierrehumbert \(2014\)](#)). These parameters can be constrained by $\text{SNR} = 10$ observations in 20% bandpasses in the same observations required to observe O_2 at $0.76 \mu\text{m}$, H_2O at $0.9 \mu\text{m}$, and CH_4 at $1.65 \mu\text{m}$ (assuming $R = 140$ in the visible and $R = 70$ in the NIR), possibly allowing us to derive this critical information “for free” during other observations searching for biosignatures and signs of habitability ([Young et al. 2024](#)). Fig. 18 shows retrievals of atmospheric pressure and surface temperature from [Young et al. \(2024\)](#). The temperature information is retrieved from temperature-dependency of opacities, mainly H_2O , while the pressure information comes from pressure-dependency of opacities.

Fig. 19 and Fig. 20 summarize the requirements for detecting atmospheric gases. Additional work, beyond the scope of this activity, will be required to fill in table cells labeled “TBD,” but these are included here to guide future work. The given wavelengths are near the centers of the absorption bands. Each feature has a finite width, which

will depend on concentration (column densities) and other factors. To adequately retrieve the gas in question, it is important to capture both sides of the continuum near the band (e.g., a buffer of $\sim 0.1\text{--}0.15 \mu\text{m}$ in the NIR). For example, to capture the $1.6 \mu\text{m}$ CO_2 band, it is important to extend the spectrum to $1.7 \mu\text{m}$. To capture the $1.65 \mu\text{m}$ CH_4 band, it is useful to extend the spectrum $1.8 \mu\text{m}$.

6. Concluding Remarks

The search for life beyond the solar system is the most ambitious goal of any NASA mission ever. Success in this endeavor would be one of the most significant discoveries in human history. The astrobiology community has provided a clear map of how to conduct this search in a way that maximizes our likelihood of success. We now await the tool that can conduct this search rigorously.

REFERENCES

Arney, G., Domagal-Goldman, S. D., & Meadows, V. S. 2018, [Astrobiology](#), 18, 311

short wavelength cutoff (μm):	0.200			0.240			0.250			0.264			0.288			0.348		
SNR	10	20	40	10	20	40	10	20	40	10	20	40	10	20	40	10	20	40
Proterozoic Earth (1% present level of O₂)	Sufficient to contextualize O ₃ biosig			Sufficient to contextualize O ₃ biosig			Sufficient to contextualize O ₃ biosig			Sufficient to contextualize O ₃ biosig			Insufficient to contextualize O ₃ biosig			Insufficient to contextualize O ₃ biosig		
O ₃	1.4 dex	1.0 dex	0.9 dex	1.6 dex	1.3 dex	1.2 dex	1.6 dex	1.3 dex	1.3 dex	1.5 dex	1.2 dex	1.2 dex	ET	ET	ET	NC	NC	NC
Proterozoic Earth (0.1% present level of O₂)	Sufficient to contextualize O ₃ biosig			Sufficient to contextualize O ₃ biosig			Sufficient to contextualize O ₃ biosig			Sufficient to contextualize O ₃ biosig			Insufficient to contextualize O ₃ biosig			Insufficient to contextualize O ₃ biosig		
O ₃	0.6 dex	0.52 dex	0.57 dex	1.2 dex	1.0 dex	0.8 dex	1.2 dex	1.2 dex	0.9 dex	1.2 dex	1.1 dex	1.0 dex	ET	ET	1.4 dex	NC	NC	NC
High SO₂ Proterozoic Earth (1% present level of O₂)	Sufficient to contextualize O ₃ biosig			Sufficient to contextualize O ₃ biosig			Sufficient to contextualize O ₃ biosig			Insufficient to contextualize O ₃ biosig			Insufficient to contextualize O ₃ biosig			Insufficient to contextualize O ₃ biosig		
O ₃	1.6 dex	1.2 dex	0.9 dex	1.6 dex	1.3 dex	1.2 dex	1.6 dex	1.3 dex	1.2 dex	ET	1.3 dex	1.2 dex	ET	ET	ET	NC	NC	NC
SO ₂	NC	NC	NC	NC	NC	NC	NC	NC	NC	NC	NC	NC	NC	NC	NC	NC	NC	NC
High SO₂ Proterozoic Earth (0.1% present level of O₂)	Sufficient to contextualize O ₃ biosig			Sufficient to contextualize O ₃ biosig			Sufficient to contextualize O ₃ biosig			Sufficient to contextualize O ₃ biosig			Insufficient to contextualize O ₃ biosig			Insufficient to contextualize O ₃ biosig		
O ₃	0.6 dex	0.5 dex	1.0 dex	1.0 dex	0.8 dex	0.7 dex	0.9 dex	0.5 dex	1.1 dex	0.9 dex	0.6 dex	1.3 dex	ET	ET	ET	NC	NC	NC
SO ₂	NC	NC	ET	NC	NC	10 ⁻⁸ UL	NC	NC	10 ⁻⁸ UL	NC	NC	10 ⁻⁸ UL	NC	NC	NC	NC	NC	NC
SUMMARY:	Sufficient for UV O ₃ detections			Sufficient for UV O ₃ detections			Sufficient for UV O ₃ detections			Marginal for UV O ₃ detections			Insufficient for UV O ₃ detections			Insufficient for UV O ₃ detections		

Fig. 16.— Summary of simulated retrievals showing the extent to which different short wavelength cutoffs enable characterization of Earth-through-time biosignatures, specifically O₃ and its potential spectral contaminant SO₂. Columns denote shortwave cutoffs and assumed SNRs (R=7), whereas rows represent different atmospheric compositions assumed for the Earth through time (abundances in parentheses). Each grid cell denotes the abundance constraint from a reflected light retrieval using the rfast spectral retrieval model (Robinson & Salvador 2023). Green grid cells show detections with abundance constraints, yellow grid cells represent upper limits that are useful for contextualizing biosignatures or ruling out known false positive scenarios, whereas red grid cells represent either no constraints (NC) or upper limits with extended tails (ET) that provide no useful contextual information for ruling out biosignature false negatives or assessing habitability. We find a short wavelength cutoff of ~0.25 μm is necessary for contextualizing Earth-like biosignatures throughout Earth’s evolution. Results based on simulations by Amber Young.

Arney, G., Domagal-Goldman, S. D., Meadows, V. S., et al. 2016, *Astrobiology*, **16**, 873

Arney, G. N. 2019, *The Astrophysical Journal Letters*, **873**, L7

Arney, G. N., Meadows, V. S., Domagal-Goldman, S. D., et al. 2017, *ApJ*, **836**, 49

Bell, E. A., Boehnke, P., Harrison, T. M., et al. 2015, *Proceedings of the National Academy of Science*, **112**, 14518

Buick, R. 2007, Did the Proterozoic ‘Canfield Ocean’cause a laughing gas greenhouse?, Wiley Online Library

Catling, D. C., KiangNancy, Y., RobinsonTyler, D., et al. 2018, *Astrobiology*

Chapman, S. 1930, *The London, Edinburgh, and Dublin Philosophical Magazine and Journal of Science*, **10**, 369

Damiano, M., Hu, R., & Mennesson, B. 2023, *The Astronomical Journal*, **166**, 157

Domagal-Goldman, S. D., Meadows, V. S., Claire, M. W., et al. 2011, *Astrobiology*, **11**, 419

Etiope, G., & Sherwood Lollar, B. 2013, *Reviews of Geophysics*, **51**, 276

Gao, P., Hu, R., Robinson, T. D., et al. 2015, *The Astrophysical Journal*, **806**, 249

Grenfell, J. L., Gebauer, S., Paris, P. v., et al. 2014, *Planetary and Space Science*, **98**, 66

Hall, S., Krissansen-Totton, J., Robinson, T., et al. 2023, *The Astronomical Journal*, **166**, 254

Harrison, T. M., Blichert-Toft, J., Müller, W., et al. 2005, *Science*, **310**, 1947

Hitchcock, D. R., & Lovelock, J. E. 1967, *Icarus*, **7**, 149

Hu, R., Seager, S., & Bains, W. 2013, *The Astrophysical Journal*, 769, 6

Kaltenegger, L. 2017, *Annual Review of Astronomy and Astrophysics*, 55, 433

Kasting, J. F. 2014, *Treatise on Geochemistry*, 6, 157

Kharecha, P., Kasting, J., & Siefert, J. 2005, *Geobiology*, 3, 53

Knowles, R. 1982, *Microbiological reviews*, 46, 43

Kopparapu, R. K., Ramirez, R., Kasting, J. F., et al. 2013, *The Astrophysical Journal*, 765, 131

Kriessansen-Totton, J., Bergsman, D. S., & Catling, D. C. 2016, *Astrobiology*, 16, 39

Kriessansen-Totton, J., Fortney, J. J., Nimmo, F., et al. 2021, *AGU Advances*, 2, e2020AV000294

Kriessansen-Totton, J., Olson, S., & Catling, D. C. 2018, *Science advances*, 4, eaao5747

Kriessansen-Totton, J., Thompson, M., Galloway, M. L., et al. 2022, *Nature Astronomy*, 6, 189

Latouf, N., Mandell, A. M., Villanueva, G. L., et al. 2023a, *The Astronomical Journal*, 166, 129

—. 2023b, *The Astronomical Journal*, 167, 27

Loftus, K., Wordsworth, R. D., & Morley, C. V. 2019, *The Astrophysical Journal*, 887, 231

Lustig-Yaeger, J., Meadows, V. S., Mendoza, G. T., et al. 2018, *The Astronomical Journal*, 156, 301

Lyons, T. W., Diamond, C. W., Planavsky, N. J., et al. 2021, *Astrobiology*, 21, 906

Lyons, T. W., Reinhard, C. T., & Planavsky, N. J. 2014, *Nature*, 506, 307

Meadows, V., Graham, H., Abrahamsson, V., et al. 2022, *arXiv preprint arXiv:2210.14293*

Meadows, V. S. 2017, *Astrobiology*, 17, 1022

Morgan, R., Savransky, D., Turmon, M., et al. 2024, in *Space Telescopes and Instrumentation 2024: Optical, Infrared, and Millimeter Wave*, Vol. 13092, SPIE, 1836–1854

National Academies of Sciences, Engineering, and Medicine. 2021, *Pathways to Discovery in Astronomy and Astrophysics for the 2020s* (The National Academies Press)

Nutman, A. P., Bennett, V. C., Friend, C. R. L., et al. 2016, *Nature*, 537, 535

Olson, S. L., Reinhard, C. T., & Lyons, T. W. 2016, *Proceedings of the National Academy of Sciences*, 113, 11447

Olson, S. L., Schwierman, E. W., Reinhard, C. T., et al. 2018, *The Astrophysical Journal Letters*, 858, L14

Pavlov, A., & Kasting, J. 2002, *Astrobiology*, 2, 27

Pavlov, A. A., Kasting, J. F., Brown, L. L., et al. 2000, *Journal of Geophysical Research: Planets*, 105, 11981

Pinto, R., Weigelhofer, G., Brito, A. G., et al. 2021, *PeerJ*, 9, e10767

Planavsky, N. J., Reinhard, C. T., Wang, X., et al. 2014, *science*, 346, 635

Pohorille, A., & Pratt, L. R. 2012, *Origins of Life and Evolution of Biospheres*, 42, 405

Ranjan, S., Schwierman, E. W., Harman, C., et al. 2020, *ApJ*, 896, 148

Ranjan, S., Schwierman, E. W., Leung, M., et al. 2023, *The Astrophysical Journal Letters*, 958, L15

Reinhard, C. T., Olson, S. L., Schwierman, E. W., et al. 2017, *Astrobiology*, 17, 287

Robinson, T. D., Meadows, V. S., & Crisp, D. 2010, *The Astrophysical Journal Letters*, 721, L67

Robinson, T. D., & Reinhard, C. T. 2018, *Planetary astrobiology*, 379

Robinson, T. D., & Salvador, A. 2023, *The Planetary Science Journal*, 4, 10

Sagan, C., Thompson, W. R., Carlson, R., et al. 1993, *Nature*, 365, 715

Sauterey, B., Charnay, B., Affholder, A., et al. 2020, *Nature communications*, 11, 2705

Schwierman, E. W., Reinhard, C. T., Olson, S. L., et al. 2019, *The Astrophysical Journal*, 874, 9

Schwierman, E. W., Meadows, V. S., Domagal-Goldman, S. D., et al. 2016, *The Astrophysical Journal Letters*, 819, L13

Schwierman, E. W., Kiang, N. Y., Parenteau, M. N., et al. 2018, *Astrobiology*, 18, 663

Schwierman, E. W., Olson, S. L., Pidhorodetska, D., et al. 2022, *The Astrophysical Journal*, 937, 109

Seager, S., Bains, W., & Petkowski, J. 2016, *Astrobiology*, 16, 465

Seager, S., Schrenk, M., & Bains, W. 2012, *Astrobiology*, 12, 61

Segura, A., Kasting, J. F., Meadows, V., et al. 2005, *Astrobiology*, 5, 706

Segura, A., Krelove, K., Kasting, J. F., et al. 2003, *Astrobiology*, 3, 689

Tabataba-Vakili, F., Grenfell, J., Grießmeier, J.-M., et al. 2016, *Astronomy & Astrophysics*, 585, A96

Thompson, M. A., Kriessansen-Totton, J., Wogan, N., et al. 2022, *Proceedings of the National Academy of Sciences*, 119, e2117933119

Tilley, M. A., Segura, A., Meadows, V., et al. 2019, *Astrobiology*, 19, 64

Tokadjian, A., Hu, R., & Damiano, M. 2024, *The Astronomical Journal*, 168, 292

Trainer, M. G., Pavlov, A. A., DeWitt, H. L., et al. 2006, *Proceedings of the National Academy of Sciences*, 103, 18035

Tuchow, N. W., Stark, C. C., & Mamajek, E. 2024, *The Astronomical Journal*, 167, 139

Ueno, Y., Yamada, K., Yoshida, N., et al. 2006, *Nature*, 440, 516

Weiss, M. C., Sousa, F. L., Mrnjavac, N., et al. 2016, *Nature microbiology*, 1, 1

Woese, C. R., & Fox, G. E. 1977, *Proceedings of the National Academy of Sciences*, 74, 5088

Wogan, N. F., & Catling, D. C. 2020, *The Astrophysical Journal*, 892, 127

Wogan, N. F., Catling, D. C., Zahnle, K. J., et al. 2023, *PSJ*, 4, 169

Wolfe, J. M., & Fournier, G. P. 2018, *Nature ecology & evolution*, 2, 897

Wordsworth, R., & Pierrehumbert, R. 2014, *The Astrophysical Journal Letters*, 785, L20

Young, A. V., Crouse, J., Arney, G., et al. 2024, *The Planetary Science Journal*, 5, 7

Zahnle, K., Claire, M., & Catling, D. 2006, *Geobiology*, 4, 271

Zahnle, K., Schaefer, L., & Fegley, B. 2010, *Cold Spring Harbor perspectives in biology*, 2, a004895

Zerkle, A. L., Claire, M. W., Domagal-Goldman, S. D., et al. 2012, *Nature Geoscience*, 5, 359

Long wavelength cutoff (μm):	1.5			1.6			1.7			1.8			2.0		
SNR	10	20	40	10	20	40	10	20	40	10	20	40	10	20	40
Phanerozoic Earth	Insufficient to contextualize O_2/O_3 biosig			Sufficient to contextualize O_2/O_3 biosig											
CO ₂ (0.1%)	10 ⁻¹ UL	10 ⁻² UL	10 ⁻² UL	10 ⁻¹ UL	10 ⁻² UL	10 ⁻² UL	10 ⁻¹ UL	10 ⁻² UL	10 ⁻² UL	10 ⁻¹ UL	10 ⁻² UL	10 ⁻² UL	10 ⁻¹ UL	10 ⁻² UL	2 dex
CH ₄ (1 ppm)	10 ⁻⁴ UL	10 ⁻⁴ UL	10 ⁻⁵ UL	10 ⁻⁴ UL	10 ⁻⁴ UL	10 ⁻⁵ UL	10 ⁻⁴ UL	10 ⁻⁴ UL	10 ⁻⁵ UL	10 ⁻⁴ UL	10 ⁻⁴ UL	10 ⁻⁵ UL	10 ⁻⁴ UL	10 ⁻⁴ UL	10 ⁻⁵ UL
CO (0.1 ppm)	NC	NC	NC	NC	10 ⁻² UL	10 ⁻² UL	10 ⁻¹ UL	10 ⁻² UL	10 ⁻² UL	10 ⁻¹ UL	10 ⁻² UL	10 ⁻² UL	10 ⁻¹ UL	10 ⁻² UL	10 ⁻² UL
Low CH₄ Proterozoic Earth	Insufficient to contextualize O_3 biosig			Sufficient to contextualize O_3 biosig											
CO ₂ (1%)	NC	1 dex	0.5 dex	NC	1 dex	0.5 dex	NC	1 dex	0.5 dex	NC	1 dex	0.5 dex	4 dex	1 dex	0.5 dex
CH ₄ (5 ppm)	10 ⁻⁴ UL	10 ⁻⁴ UL	10 ⁻⁵ UL	10 ⁻⁴ UL	10 ⁻⁴ UL	10 ⁻⁵ UL	10 ⁻⁴ UL	10 ⁻⁴ UL	10 ⁻⁵ UL	10 ⁻⁴ UL	10 ⁻⁴ UL	10 ⁻⁵ UL	10 ⁻⁴ UL	10 ⁻⁴ UL	10 ⁻⁵ UL
CO (0.1 ppm)	NC	NC	NC	NC	NC	10 ⁻² UL	NC	NC	10 ⁻² UL	NC	10 ⁻¹ UL	10 ⁻² UL	NC	10 ⁻¹ UL	10 ⁻² UL
High CH₄ Proterozoic Earth	Insufficient to contextualize O_3/CH_4 biosig			Insufficient to contextualize O_3/CH_4 biosig			Sufficient to contextualize O_3/CH_4 biosig			Sufficient to contextualize O_3/CH_4 biosig			Sufficient to contextualize O_3/CH_4 biosig		
CO ₂ (1%)	NC	2 dex	1 dex	NC	2 dex	1 dex	NC	2 dex	1 dex	NC	2 dex	1 dex	NC	2 dex	1 dex
CH ₄ (100 ppm)	NC	2 dex	1 dex	NC	2 dex	1 dex	3 dex	2 dex	1 dex	3 dex	2 dex	1 dex	3 dex	2 dex	1 dex
CO (0.1 ppm)	NC	NC	NC	NC	10 ⁻¹ UL	10 ⁻² UL									
Late Archean Earth (high CH₄)	Insufficient to contextualize CH ₄ biosig			Sufficient to contextualize CH ₄ biosig			Sufficient to contextualize CH ₄ biosig			Sufficient to contextualize CH ₄ biosig			Sufficient to contextualize CH ₄ biosig		
CO ₂ (5%)	2 dex	2 dex	1 dex	2 dex	2 dex	1 dex	2 dex	2 dex	1 dex	2 dex	2 dex	1 dex	2 dex	2 dex	1 dex
CH ₄ (0.5%)	2 dex	1 dex	1 dex	2 dex	1 dex	0.5 dex	2 dex	1 dex	0.5 dex	2 dex	1 dex	0.5 dex	2 dex	1 dex	0.5 dex
CO (500 ppm)	NC	NC	NC	10 ⁻¹ UL	10 ⁻¹ UL	10 ⁻² UL	10 ⁻¹ UL	10 ⁻¹ UL	10 ⁻² UL	10 ⁻¹ UL	10 ⁻¹ UL	10 ⁻² UL	10 ⁻¹ UL	10 ⁻¹ UL	10 ⁻² UL
Early Archean Earth (low CH₄)	Insufficient to contextualize CH ₄ biosig			Sufficient to contextualize CH ₄ biosig			Sufficient to contextualize CH ₄ biosig			Sufficient to contextualize CH ₄ biosig			Sufficient to contextualize CH ₄ biosig		
CO ₂ (20%)	2 dex	1 dex	1 dex	2 dex	1 dex	1 dex	2 dex	1 dex	1 dex	2 dex	1 dex	1 dex	2 dex	1 dex	1 dex
CH ₄ (500 ppm)	2 dex	1 dex	1 dex	2 dex	1 dex	1 dex	2 dex	1 dex	1 dex	2 dex	1 dex	1 dex	2 dex	1 dex	1 dex
CO (50 ppm)	NC	NC	NC	10 ⁻¹ UL	10 ⁻¹ UL	10 ⁻¹ UL	10 ⁻¹ UL	10 ⁻¹ UL	10 ⁻¹ UL	10 ⁻¹ UL	10 ⁻¹ UL	10 ⁻¹ UL	10 ⁻¹ UL	10 ⁻¹ UL	10 ⁻¹ UL
SUMMARY:	Insufficient for characterizing Earth-thru time.			Marginal(?) for characterizing Earth-thru time.			Sufficient for characterizing Earth-thru time.			Sufficient for characterizing Earth-thru time.			Sufficient for characterizing Earth-thru time.		

Fig. 17.— Summary of simulated retrievals showing the extent to which different long wavelength cutoffs enable characterization of Earth-through-time biosignatures. Columns denote longwave cutoffs and assumed SNRs (R=7 UV, R=140 VIS, R=70 NIR), whereas rows represent different atmospheric compositions assumed for the Earth through time (abundances in brackets). Each grid cell denotes the abundance constraint from a reflected light retrieval using the rfast spectral retrieval model (Robinson & Salvador 2023). Green grid cells show detections with abundance constraints, yellow grid cells represent upper limits that are useful for contextualizing biosignatures or ruling out known false positive scenarios, whereas red grid cells represent either no constraints (NC) or upper limits (UL) that provide no useful contextual information for ruling out biosignature false positives or assessing habitability. We find a long wavelength cutoff of at least 1.7 μm is necessary for contextualizing Earth-like biosignatures throughout Earth's evolution. Results based on simulations by Maxwell Frissell (UW), Anna Grace Ulles (UW), and Samantha Gilbert-Janizek (UW).

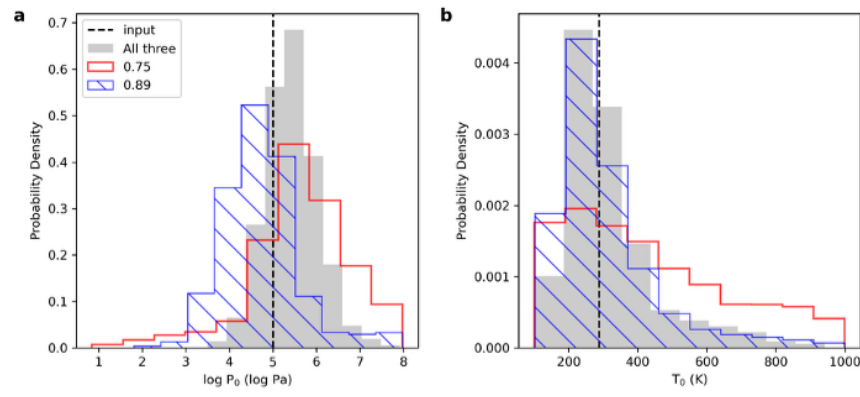


Fig. 18.— Posterior distributions for global surface pressure (left) and global temperature (right) from simulated SNR = 10 observations. Bandpass centers are indicated in the legend, and the “all three” (gray) retrieval combines information from all three bandpasses considered, which are centered on O₂, H₂O, and CH₄ features. Reproduced with permission from [Young et al. \(2024\)](#).

Desired spectral features for habitability assessment & the search for life.

SNR calculated wavelengths bolded; False positive indicators indicated with *					
Molecules or Feature	UV-VIS wavelengths (0.2 – 1.0 μm)	NIR wavelengths (1.0 – 2.5 μm)	Reason	Desired abundance & precision	Required SNR
H_2O^*	0.65, 0.72, 0.82, 0.94	1.12, 1.4, 1.85	Vital habitability indicator	1% by volume (Modern Earth), 1 dex	6 (12 for low water)
O_2	0.2, 0.63, 0.69, 0.76 (strong)	1.27	Essential modern Earth biosignature	21% by volume (Modern Earth), 1 dex	8
O_3	0.2 – 0.35 (strong), 0.5–0.7	2.48	Essential Proterozoic Earth biosignature; modern Earth biosignature	O_3 corresponding to 0.1% present atmospheric level of O_2 : 3×10^{-8} (Proterozoic Earth), 1-2 dex	10-20
CH_4	0.6, 0.79, 0.89 , 1.0	1.1, 1.4, 1.7 , 2.3	Essential Archean Earth biosignature; habitability assessment	500 ppm by volume (Archean) / 100 ppm (Proterozoic), 1 dex	10
CO^*		1.6, 2.35	CH_4 & O_2 false positive indicator;	< 10% by volume, upper limit	>10
CO_2^*		1.05, 1.21, 1.44, 1.59 , 2.0 (strong)	CH_4 & O_2 false positive indicator; habitability assessment	~1% by volume (Archean Earth), 1 dex	10 (weak) or 20 (strong)
S_8	0.2-0.5		Habitability assessment (volcanism)	Best effort	Best effort
H_2S	< 0.3		Habitability assessment (volcanism)	Best effort	Best effort
SO_2	< 0.3	2.47	Habitability assessment (volcanism)	Best effort	Best effort
H_2	0.64 – 0.66, 0.8 – 0.85		Alternative habitability assessment	Best effort	Best effort
O_4 (O_2 - O_2) *	0.345, 0.36, 0.38, 0.45, 0.48, 0.53, 0.57, 0.63	1.06, 1.27 (strong)	O_2 false positive indicator	TBD	TBD
N_2O		1.4 , 1.8 , 1.78, 2.0, 2.11 (strong), 2.26 (strong)	Alternative Proterozoic biosignature	1000 ppm (Proterozoic-like), 1 dex	20
NO_2	< 0.55	2.1, 2.4	Pollution technosignature	TBD	TBD
NH_3		1.3, 1.98, 2.3	Possible biosignature; prebiotic chemistry	TBD	TBD
Organic haze	$\lesssim 0.5$		Biosignature; habitability assessment	Best effort	Best effort
Vegetation red edge	0.6 (halophile), 0.7 (photosynthesis)		Biosignature	TBD	TBD
Ocean glint	0.8 – 0.9	1.0 – 1.05, 1.3	Habitability indicator	TBD	TBD
Rayleigh scattering	$\lesssim 0.5$		Habitability assessment	Best effort	Best effort

Fig. 19.— Desired spectral features for habitability assessment and search for life as well as calculated requirements for measurements. SNR calculated wavelengths bolded, false positive indicators indicated with *.

Observation requirement	State of the Art	Incremental Progress (Enhancing)	Substantial Progress (Enabling)	Major Progress	Breakthrough	Super Breakthrough +++
Minimum Wavelength for Spectroscopy	N/A	0.45 um	0.45 um	0.4 um	0.25 um	0.25 um
Maximum Wavelength for Spectroscopy	N/A	1.1 um	1.1 um	1.7 um	1.7 um	1.7 um
Spectral resolution	N/A	R=140 from 0.45 – 1.1 um	R=140 from 0.45 – 1.1 um	R = 140 from 0.4 to 1.1 um R = 70 from 1.1-1.7 um (TBC)	R = 7 from 0.25-0.4 R = 140 from 0.4 to 1.1 um R = 70 from 1.1-1.7 um (TBC)	R = 7 from 0.25-0.4 R = 140 from 0.4 to 1.1 um R = 70 from 1.1-1.7 um (TBC)
Signal to noise on continuum near relevant band	N/A	SNR = 6 near 0.94 um H ₂ O SNR = 8 near 0.76 um O ₂ SNR = 10 near 0.89 um CH ₄ (TBC)	SNR = 6 near 0.94 um H ₂ O SNR = 8 near 0.76 um O ₂ SNR = 10 near 0.89 um CH ₄ (TBC)	SNR = 6 near 0.94 um H ₂ O SNR = 8 near 0.76 um O ₂ SNR = 10 near 0.89 um CH ₄ (TBC) SNR > 10 near 1.59 um CO ₂ SNR > 20 near 1.6 um CO	SNR = 6 near 0.94 um H ₂ O SNR = 8 near 0.76 um O ₂ SNR = 10 near 0.89 um CH ₄ (TBC) SNR > 10 near 1.59 um CO ₂ SNR > 20 near 1.6 um CO SNR = 10 near NUV O ₃	SNR = 6 near 0.94 um H ₂ O SNR = 8 near 0.76 um O ₂ SNR = 10 near 0.89 um CH ₄ (TBC) SNR > 10 near 1.59 um CO ₂ SNR > 20 near 1.6 um CO SNR = 10 near NUV O ₃

Fig. 20.— Observational requirements to observe living worlds.